Mineralogy and Petrology (2022) 116:251–272
https://doi.org/10.1007/s00710-022-00781-3

ORIGINAL PAPER

# Geochemistry of granitoids from the Austroalpine Seckau Complex: a key for revealing the pre-Alpine evolution of the Eastern Alps

Magdalena Mandl[2] · Walter Kurz[1] · Christoph Hauzenberger[1] · Harald Fritz[1] · Stefan Pfingstl[1]

Received: 30 July 2021 / Accepted: 2 May 2022 / Published online: 19 May 2022



## Abstract
Recent studies revealed that the calc-alkaline metagranitoids of the Seckau Complex comprise both (1) a Late Cambrian to Early Ordovician and (2) a Late Devonian to Early Carboniferous (early Variscan) intrusive complex. The older rocks of the Hochreichart Plutonic Suite reflect I to S-type affinity and are peraluminous and characterized by a general decrease in $TiO_2$, $Al_2O_3$, MgO, CaO, $P_2O_5$, FeOt and MnO with increasing $SiO_2$. Chondrite-normalized rare earth element (REE) plots display a slight enrichment in light rare earth elements (LREE) relative to heavy rare earth elements (HREE) as well as negative Eu anomalies ($(Eu/Eu^*)_N = 0.15$- 0.77). The whole-rock initial $^{87}Sr/^{86}Sr$ ratios calculated back to the time of emplacement (~496 Ma) vary between 0.7056 to 0.7061. The early Variscan rocks of the Hintertal Plutonic Suite can be subdivided into (a) the meta- to peraluminous granodioritic suite of the Pletzen Pluton and (b) the peraluminous granitic suite of the Griessstein Pluton. The Pletzen Pluton shows typical magmatic fractionation trends for most of the major oxides and trace elements plotted against $SiO_2$. On a chondrite-normalized diagram, metagranitoids are strongly enriched in LREE and show no significant negative Eu anomaly. Metagranitoids of the Griessstein Pluton have a more peraluminous character and similar major and trace element fractionation trends compared to the Pletzen Pluton. However, the contents in $SiO_2$, major and trace elements clearly point towards a more evolved melt with generally lower $TiO_2$, $Al_2O_3$, MgO and CaO values and higher $K_2O$ content. Metagranitoids of the Griessstein Pluton are additionally characterized by a slight negative Eu anomaly of about 0.81 on a chondrite-normalized REE plot. Initial $^{87}Sr/^{86}Sr$ values calculated back to the time of emplacement (~353 Ma) of the Pletzen Pluton and the Griessstein Pluton vary between 0.7051—0.7061 and 0.7054—0.7063, respectively, and suggest the same magmatic source for both units. Application of rhyolite-MELTS modelling to the Hintertal Plutonic Suite revealed that the Griessstein Pluton formed by fractional crystallization (~30%) from the more primitive Pletzen Pluton. Our geochemical data from the Hochreichart Suite granitoids suggest the existence of a Late Cambrian to Early Ordovician active margin with its remnants now exposed in the Seckau Complex. The early Variscan grainitoids of the Seckau Complex are inferred as part of a magmatic arc along the southern Bohemian active continental margin that was related to the subduction of differently termed oceanic domains (Galicia-Moldanubian Ocean or Paleotethys), prior to the final collision of Gondwana and Laurussia. The general paleogeographic position of the Seckau Complex during the Variscan orogeny is considered to be south to southeast of the Bohemian Massif, adjacent to the eastern Hohe Tauern, the Schladming Tauern, and the Western Carpathians.


**Keywords** Eastern Alps · Granitoids · Geochemistry · Pre-Alpine Paleogeography

## Introduction

The Variscan orogen formed through long and diachronous convergence and collision of Gondwana lithospheric fragments with Laurussia that finally amalgamated during the Carboniferous. Individual orogenic phases are known to expand from early to mid- Devonian to Pennsylvanian times and were associated with the emplacement of numerous granitoids, which are heterogenous in terms of ages,

Editorial handling: X. Xu

✉ Walter Kurz
walter.kurz@uni-graz.at

[1] Institute of Earth Sciences, University of Graz, NAWI Graz Geocenter, Heinrichstraße 26, 8010 Graz, Austria

[2] MAPAG (Materialprüfung G.M.B.H), Industriestraße 7, 2352 Gumpoldskirchen, Austria

geochemistry, source and regional distribution (Finger et al. 1997).

The European Variscides extend from Poland to southern Iberia with distinctive exposures in the Bohemian Massif (e.g., Franke 1989, 2000; Franke and Zelazniewiez 2002; Finger et al. 2007), the French Massif Central (e.g., Santallier et al. 1994), the Armorican Massif (e.g., Ballèvre et al. 1994) and the Iberian Massif (e.g., Gómez Barreiro et al. 2006, 2007). The Alpine orogeny reworked the southern part of the Variscan orogen, but its fragments are still preserved and occur in different tectonic positions in the Alps e.g., the Aar Batholith (Helvetic unit), the Bernina Batholith, the Hohe Tauern Batholith (Sub-Penninic unit) and numerous granitoids belonging to the Austroalpine nappe system e.g., the Schladming Batholith, and the Seckau-Bösenstein Batholith (e.g., Schaltegger 1990; Schermaier et al. 1997; Eichhorn et al. 2000; von Raumer et al. 2013; Mandl et al. 2018). Along the northern front of the Alps, Cetic granitoid fragments represent early Variscan granitoids embedded in the Ultrahelveticum and the Rheno-Danubian Flysch Belt (Fig. 1) (Finger et al. 1997; Frasl and Finger 1988). Further to the east, Variscan granitoids mainly occur in the Tatric and Veporic units of the Western Carpathians which correlate with granitoids of the Austroalpine nappe system (Neubauer 1994; Broska and Uher 2001; Gaab et al. 2005; Burda et al. 2021).

In contrast to the well-studied plutons of the northern and central European Variscides, only few data exist from the re-worked intra-Alpine granitoids originating from the former southern part of the Variscan orogen. Granitoids of the Seckau Complex (Eastern Alps), now observed as metagranitoids, were generally considered to be part of these intra-Alpine Variscan intrusive suites. Recent studies, however, revealed that the metagranitoids of the Seckau Complex are part of both a late Cambrian to Early Ordovician, and Late Devonian to Early Carboniferous (early Variscan) intrusive complex (Mandl et al. 2018). While the older intrusives comprise primarily peraluminous granitoids with I- to S-type characteristics, the early Variscan granitoids represent meta- to peraluminous granitoids, which represent mostly I-type characteristics.

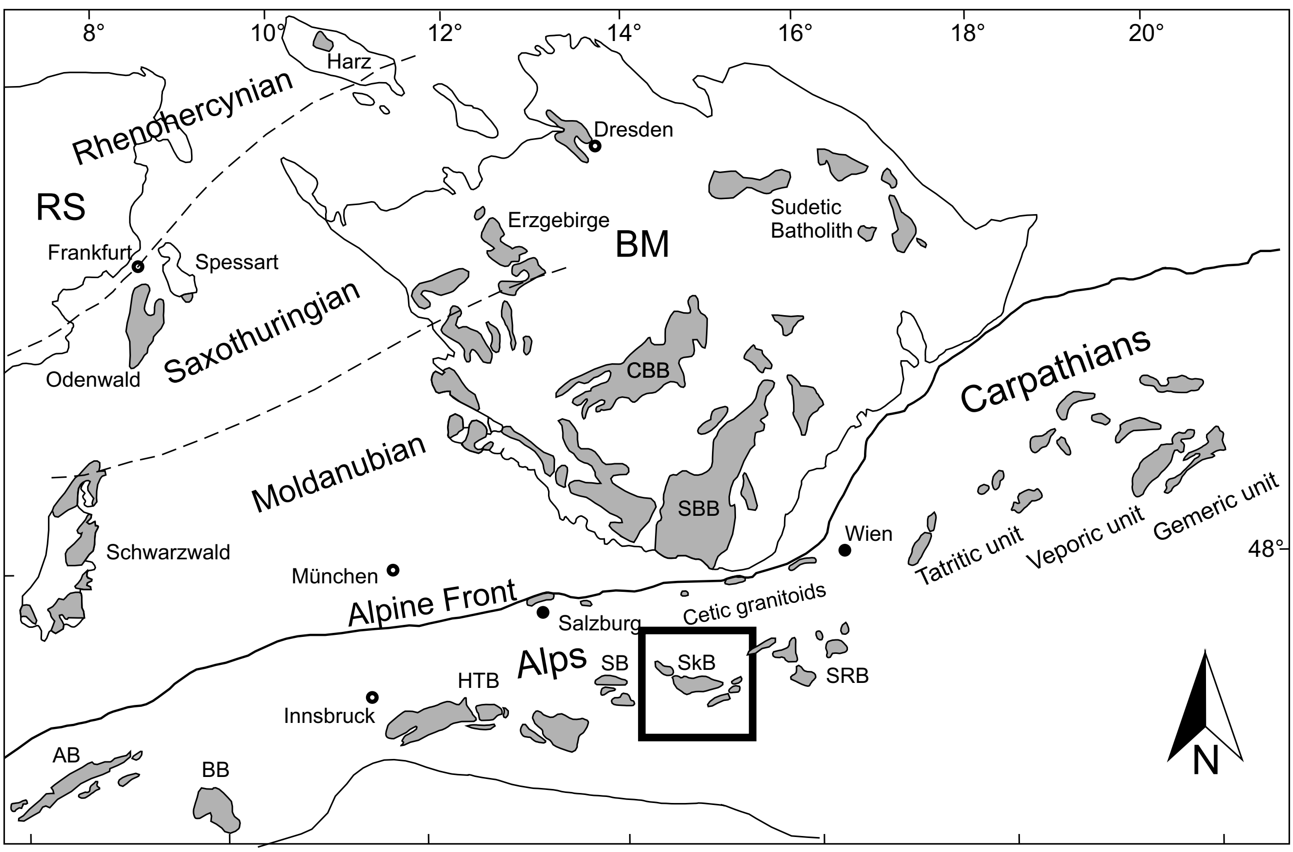


**Fig. 1** Simplified geological sketch-map showing the distribution of Variscan granitoids of central Europe (modified after Finger et al. 1997, 2003, 2009; Franěk et al. 2011) Abbreviations: AB: Aar Batholith, BB: Bernina Batholith, BM: Bohemian Massif, CBB: Central Bohemian Batholith, HTB: Hohe Tauern Batholith, SB: Schladming Batholith, SkB: Seckau-Bösenstein Batholith, RS: Rheinisches Schiefergebirge, SBB: South Bohemian Batholith, RB: Raabalpen Batholith; the Raabalpen Batholith had recentkly been dated as post-Variscan (Middle to Late Permian; e.g. Yuan et al. 2020)

Based on the geochronological results of Mandl et al. (2018) new geochemical data as well as recalculated Sr isotope data from literature (Pfingstl et al. 2015) were used in order to (1) better understand and constrain the evolution of Variscan magmatism and magmatic differentiation of the Seckau Complex and (2) characterize the older late Cambrian to Early Ordovician plutonic suite of the Seckau Complex.

## Geological setting

The nappe systems of the Eastern Alps (Fig. 1) comprise widely exposed pre-Alpine basement units that are covered by Upper Carboniferous to Eocene sedimentary sequences (for summary, see Schmid et al. 2004).

Large parts of Variscan and pre-Variscan crust, including its sedimentary cover, were incorporated into the Alpine orogen during the continuous convergence of the African and European continental plates from Late Jurassic times onwards. Several oceanic basins and microcontinents were involved in this collision event at different times (Schmid et al. 2004). The Eastern Alps (Figs. 1, and 2) are basically the product of two orogenic collision events: (1) the Eo-Alpine event (Frank 1987) and (2) the Alpine event (e.g., Froitzheim et al. 1996). The Eo-Alpine event is basically related to the closure of the Meliata Ocean. The subsequent Alpine event (Late Cretaceous to Paleogene) followed the subduction of the Penninic oceans (Piemont-Ligurian and Valais Ocean), due to the collision of Europe and Adria (Froitzheim et al. 1996; Schmid et al. 2004; Schuster 2004). Accordingly, the nappe stack in the (Eastern) Alps can be subdivided into three main structural units: (1) the Helvetic realm and sub-Penninic nappes, representing the former southern European continental margin, (2) the Penninic nappes, comprising oceanic (Piemont-Ligurian Ocean and Valais Ocean) and continental crust (e.g., Brianconnais) and (3) the Austroalpine nappes, representing continental crust from the northern part of former Adria (Fig. 2a) (Schuster 2003; Schmid et al. 2004; Froitzheim et al. 2008).

Basement units within the Austroalpine nappe system consist of Cadomian continental crust with Paleozoic metasedimentary sequences, and magmatic rocks related to rifting and subduction processes lasting until Carboniferous times (for summary, see von Raumer and Neubauer (1993); von Raumer et al. 2013). During the Variscan orogeny large parts of this crust were affected by metamorphic overprint and synorogenic magmatism.

The Lower Austroalpine basically derived from the northern continental margin of Adria facing towards the Piemont-Ligurian Ocean (e.g., Schmid et al. 2004). The Upper Austroalpine Subunit, widely exposed in the Eastern Alps, is mainly shaped by the Eo-Alpine collision event (Eo-Alpine as term for the Early Cretaceous to early Late Cretaceous orogeny). It comprises Paleozoic and Mesozoic cover units along the northern margin of the Eastern Alps (Northern Calcareous Alps) and Paleozoic metasediments and metavolcanics of the Graywacke Zone. In the central and southern part, pre-Alpine crystalline basement units such as (from bottom to top) the Silvretta-Seckau-, the Koralpe-Wölz-, the Ötztal-Bundschuh- and Drauzug-Gurktal Nappe Systems are mostly covered by Late Carboniferous-Permian to Mesozoic metasediments (Schmid et al. 2004; Froitzheim et al. 2008).

The Silvretta-Seckau Nappe System (Fig. 2), being the focus of this study, consists of a pre-Alpine metamorphic and magmatic basement and remnants of Carboniferous to Triassic cover sequences. The Seckau Nappe, as part of the Silvretta-Seckau Nappe System, was overprinted by subgreenschist to greenschist facies metamorphic conditions during the Eo-Alpine event (Schuster et al. 2013; Faryad and Hoinkes 2003), as indicated by Rb–Sr biotite ages in the range of 85 to 82 Ma (Pfingstl et al. 2015). The main area of exposure extends from the Bösenstein Massif (Pölsenstein Massif in Metz 1976) to the Seckau Tauern (Fig. 2). The Seckau Nappe comprises several pre-Alpine basement complexes (Fig. 2b): Seckau Complex, Amering Complex, Gleinalm/Gleinalpe and Rennfeld Complex as well as Permian to Lower Triassic metasediments summarized as Rannach-Formation (Metz 1967; Flügel and Neubauer 1984; Faryad and Hoinkes 2001; Gaidies et al. 2006; Pfingstl et al. 2015). The Seckau Complex is dominated by paragneisses (partly migmatitic) and micaschists being intruded by large volumes of meta- to peraluminous granitoids. Together, the granitoids make up about 90% of the Seckau Complex (Schermaier et al. 1997). Whereas the paleogeographic and tectonic position of these basement complexes during Alpine evolutionary steps is ascertained, their plate tectonic arrangement during Cambrian and Late Devonian / Mississippian times remains unclear and is focus of this study.

Recent studies revealed a more distinct subdivision of the Seckau Complex based on petrological, geochemical and geochronological data (Mandl et. al. 2018) (Fig. 3). The Glaneck Metamorphic Suite comprises paragneisses with U–Pb ages of originally detrital zircons in the range from Neoarchean (ca. 2.7 Ga) to Ediacaran (ca. 559 Ma) with distinct frequency peaks between ca. 572 ± 7 Ma and 559 ± 11 Ma. Highly fractionated peraluminous granites of the Hochreichart Suite indicate a magmatic event between 508 ± 9 Ma and 486 ± 9 Ma that may also have caused migmatisation of distinct domains in the paragneisses of the Glaneck Metamorphic Suite. The Hintertal Plutonic Suite displays a second intrusion event ranging from 365 ± 8 Ma to 343 ± 12 Ma and comprises meta- to peraluminous granodiorites (Pletzen Pluton) as well as peraluminous granites (Griessstein Pluton).

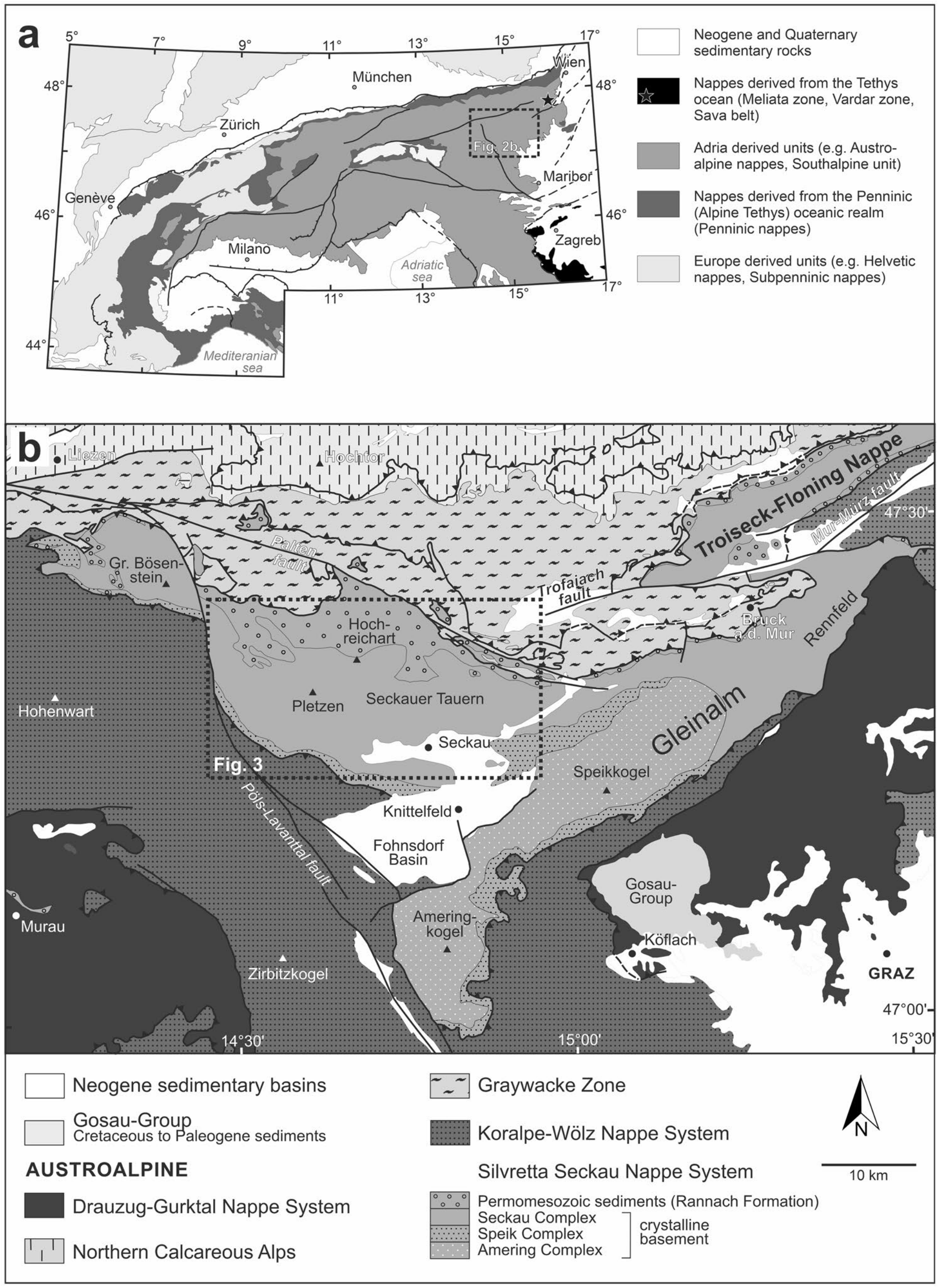


**Fig. 2** (**a**) Overview map showing the paleogeographic origin of the main tectonic units of the Alps after Schmid et al. (2004). The dotted square indicates the location of the map shown in Fig. 2b. (**b**) Simplified geological map of the Austroalpine basement units to the east of the Tauern Window (modified after Mandl et al. 2018). The study area (part of the Seckau Nappe System) is marked with a dotted rectangle

## Analytical methods

Forty-eight samples, up to 10 kg each. representing the metagranitoids of the Seckau Complex were taken and analyzed for this study. All analyses were conducted at the Institute of Earth Sciences, NAWI Graz Geocenter, University of Graz, Austria. All samples were cut with a rock saw and the thin sections were prepared and examined by optical microscopy. The remaining major parts of the samples were crushed and for major and trace element analysis, a representative aliquot was milled to a homogenous powder in a tungsten carbide vibratory disc mill. Before further preparation the powder was dried at 105 °C for 2 h. 1 g of the dried powder was used for Loss on ignition (LOI) by heating the samples to 1030 °C for 1 h. Fused glass discs of ~ 4 cm diameter, were produced with 1 g of rock powder and a mixture of 4.62 g of lithium tetraborate and 2.38 g of lithium metaborate powder.

Major- and selected trace- element concentrations (Rb, Sr, Zr and Ba) of whole-rock samples were determined by a Bruker Pioneer S4 X-ray fluorescence (XRF) spectrometer on fused glass discs (see Mandl et al. 2018 for details). The reproducibility of major elements was better than 1% and for

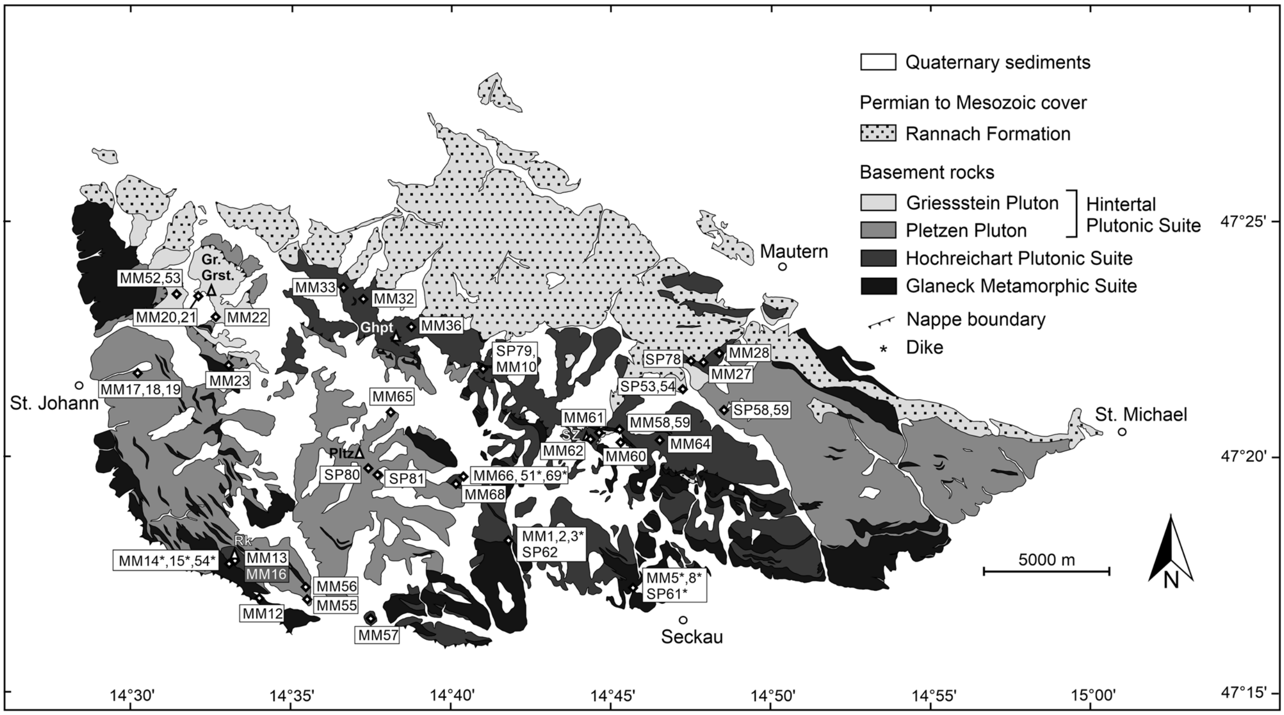


**Fig. 3** Simplified geological map of the Seckau Complex (modified after Mandl et al. 2018) to the northeast of the Mur valley showing the locations of the sampled metagranitoids. Abbreviations: Ghpt: Geierhaupt, Gr. Grst: Großer Griessstein, Pltz: Pletzen, Rk: Rosenkogel, SZ: Seckauer Zinken. Sample MM16 is a reference sample for the chemical composition of paragneisses

trace elements within 3–5%. Detection limits for major, minor and trace elements determined by XRF are 0.01 wt%, 0.005 wt% and 20 µg/g, respectively. International standards as e.g., AC-E, MA-N, GSP-2 were routinely measured to ensure analytical accuracy. Trace elements and rare earth elements were determined by inductively coupled plasma mass spectrometry (ICP-MS, Agilent 7500) at the Institute for Analytical Chemistry, University of Graz (Austria). For the analytical procedure about 50 mg of powdered sample were placed in a Teflon beaker and dissolved in concentrated nitric ($HNO_3$) and hydrofluoric (HF) acid mixture with a volumetric ratio of 1:2. The uncapped beakers were placed on a hot plate at 100 °C for 30 min, then tightly capped and returned to the hot plate at 180 °C for at least 48 h. After dissolution and evaporation, samples were extracted with 7.5 N $HNO_3$ and diluted 1500 times. The analytical results for standards GSP-2, JR-2, BCR-2, BHVO-2 were for most elements within the specified uncertainty. Detection limits for trace and rare earth elements determined by ICP-MS are 0.05 µg/g.

## Sample description

Sample locations of the Seckau Complex metagranitoids are displayed in Fig. 3; coordinates of sample sites are listed in supplementary Table S1. Based on field observations and petrographic characteristics, the granitoid intrusions of the Seckau Complex, now mostly observed as metagranitoids, can be distinguished into two plutonic suites.

### Hochreichart plutonic suite

The first suite, termed Hochreichart Plutonic Suite (Mandl et al. 2018), comprises granite gneisses and slightly deformed granites as well as subordinate granodioritic gneisses with U–Pb zircon ages in the range between 508 ± 9 Ma and 486 ± 9 Ma (Mandl et al. 2018). These plutons predominantly occur in the northern, northeastern- and southern parts of the Seckau Complex (MM1, MM2, MM10, MM27, MM28, MM32, MM33, MM36, MM58, MM59, SP78, SP79), (Fig. 3). Undeformed to slightly deformed granites (MM60, MM61, MM64, MM68) appear in the field as felsic rocks compared to the slightly darker granite gneisses in this area.

The granite gneisses of the Hochreichart Plutonic suite usually display S-type to minor I-type affinity. The magmatic mineral assemblage predominantly consists of quartz, K-feldspar, plagioclase (with partial saussuritization), muscovite, biotite (orange colored). Zircon, apatite, garnet and opaque phases are common as accessory minerals. Chlorite, titanite, epidote/zoisite, and calcite formed during Eo-Alpine low to medium grade metamorphic overprint. Large

K-feldspar idiocrysts, up to several cm in size, as well as quartz aggregates occur in a fine-grained groundmass of equigranular quartz and feldspar (Fig. 4a, b). The dominance of muscovite over biotite and a hiatial texture are observed in most samples. The modal composition comprises approximately 35–40 vol% quartz, 25–20 vol% K-feldspar, 20 vol% plagioclase, 5 vol% biotite (brownish to orange colored) and around 15–20 vol% muscovite.

In the southern region of the Seckau Complex granite gneisses are characterized by a pronounced penetrative foliation, medium-grained mica (up to a few millimeters grain size), and the dominance of biotite over muscovite. These granite gneisses (e.g., MM1, MM2) are mostly composed of approximately 35–40 vol% quartz, 20–28 vol% K-feldspar, 20 vol% plagioclase, 15–20 vol% biotite (brownish to orange colored) and around 5 vol% muscovite. Muscovite-bearing granite gneisses (e.g., SP78) differ from adjacent granite gneisses due to the absence of biotite. The undeformed to slightly deformed granites are usually medium- to coarse-grained with equigranular textures and consist of quartz, feldspar and minor mica, mostly muscovite. The modal composition comprises approximately 35–40 vol% quartz, 25–20 vol% K-feldspar, 20 vol% plagioclase and around 15–20 vol% muscovite.

### Hintertal plutonic suite

The Late Devonian to Mississippian (365 ± 8 Ma to 343 ± 12 Ma) Hintertal Plutonic Suite (Mandl et al. 2018) can be subdivided into (a) the Pletzen Pluton consisting of metagranitoids with I-type characterictics (samples: MM12, MM17, MM18, MM19, MM23, MM55, MM56, MM65, SP58, SP59, SP80 and SP81) and (b) the Griessstein Pluton, comprising fine-grained metagranitoids with S-type to minor I-type affinity (samples: MM20, MM21, MM22, MM52, MM53, SP53 and SP54) (Mandl et. al. 2018). The Pletzen Pluton makes up about 90% of the Hintertal Plutonic Suite and predominantly covers the central, western and some southern parts of the Seckau Complex, while the Griessstein Pluton only occurs in small domains close to the Hochreichart Plutonic Suite. The Hintertal Plutonic Suite can be clearly distinguished from the Hochreichart Plutonic Suite and comprises besides granitic rocks predominantly granodiorites and quartz monzodiorites. In the field most of these rocks appear blocky, coarse-grained and weakly foliated.

The metagranitoids consist mainly of plagioclase, quartz, K-feldspar, biotite (olive- to moss-green colored), muscovite and large titanite crystals with an average grain-size of 200–500 µm (Fig. 4c, d). Biotite is usually more common than muscovite and K-feldspar is mostly completely altered to sericite but its original shape is usually still preserved. In some cases, feldspar also shows poikilitic texture. The most basic rock within this suite, a coarse-grained hornblende-biotite bearing monzodiorite gneiss MM12, comprises about 31 vol% biotite, 25 vol% hornblende, 22 vol% quartz and 21 vol% plagioclase (Fig. 4e, f). Slightly deformed granitoids display an equigranular texture, composed of intensively sericitized feldspar and olive-green colored biotite (e.g., MM55 and MM65: 60 vol% plagioclase, 20 vol% quartz, 14–8 vol% biotite, 10–5 vol% K-feldspar). Strongly deformed granitoids show an inequigranular texture with fewer and smaller sized plagioclase (e.g., MM56). Biotite-granite gneisses (e.g., MM18, MM23) are characterized by a mineral content of about 38 vol% plagioclase, 32 vol% quartz, 21 vol% K-feldspar and approximately 7 vol% biotite. The metagranitoids of the Griessstein Pluton (MM20, MM21, MM52, MM53, SP53, SP54) can be clearly distinguished from the Pletzen Pluton due to their fine-grained texture, their dominance of K-feldspar and muscovite; olive- to moss-green colored biotite and large titanite crystals are almost absent (Fig. 4g, h). The modal composition comprises approximately 35 vol% quartz, 25–20 vol% K-feldspar, 30–25 vol% plagioclase and around 12–10 vol% muscovite.

**Fig. 4** Representative photomicrographs of (**a**, **b**) granite gneiss MM27 from the Hochreichart Plutonic Suite, (**c**, **d**) hornblende-biotite quartz monzodiorite gneiss MM12 and (**e**, **f**) biotite granite MM18, both representative of the Pletzen Pluton (Hintertal Plutonic Suite) and (**g**, **h**) granite gneiss MM20 of the Griessstein Pluton (Hintertal Plutonic Suite). Photomicrographs on the left-hand side are shown with crossed polarizers and those on the right-hand side under parallel polarizers. All scale bars are 400 µm. Abbreviations: Bt: biotite, Hbl: hornblende, Kfs: K-feldspar, Ms: muscovite, Pl:plagioclase, Qz: quartz, Spn: sphene (titanite). Abbreviations for names of rock-forming minerals follows Whitney and Evans (2010) ▸

### Dikes

Granitic, leucogranitic and pegmatitic dikes intruded into paragneisses of the Glaneck Metamorphic Suite and metagranitoids of the Hochreichart Pluton. They show variable orientation and occur as both concordant and discordant dikes with respect to the penetrative paragneiss foliation. They are summarized in a "dike" group and are discussed separately. Sample locations are marked in Fig. 3. Fine-grained granitic occur concordantly within the paragneisses (MM14, MM15) or penetrate them discordantly (MM54). Another granitic dike (MM69) was sampled within a biotite granodiorite gneiss. MM3 represents a leucogranitic dike intruded within a granite gneiss. Similar to the granites of the Griessstein Pluton the dike rocks are characterized by a fine-grained texture with the dominance of K-feldspar and muscovite and rare biotite. They also show, compared to the Griessstein Pluton, a similar modal composition of 35–30 vol% quartz, 25–20 vol% K-feldspar, 30–25 vol%

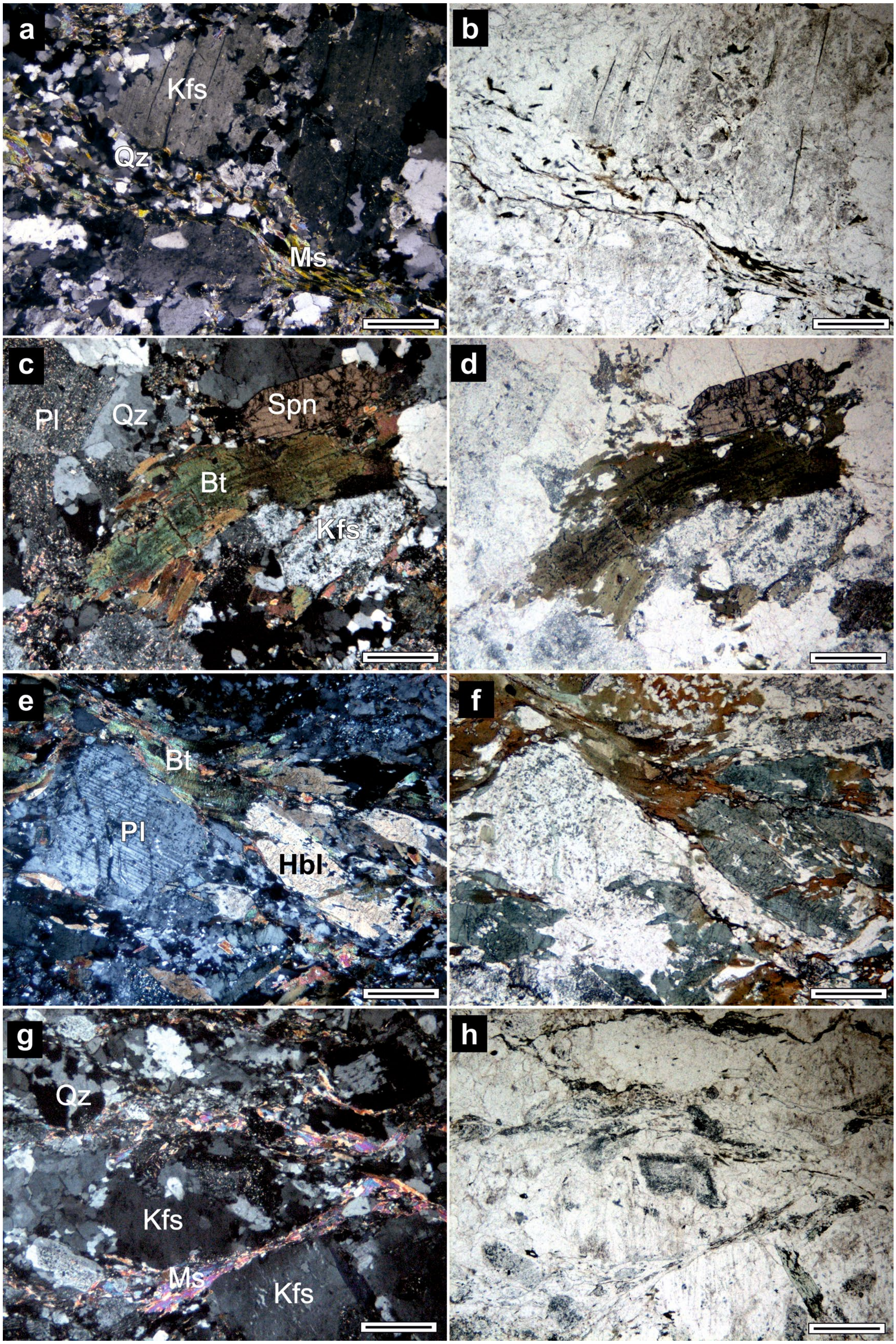
a
Kfs
Qz
Ms
b
c
Pl
Qz
Spn
Bt
Kfs
d
e
Bt
Pl
Hbl
f
g
Qz
Kfs
Ms
Kfs
h

plagioclase and around 10 vol% muscovite. Pegmatitic dikes (MM5, MM51 and SP61) crosscut paragneisses mainly discordantly. These dikes show a larger average grain size compared to the granitic dikes; the mineral assemblage is characterized by albitic plagioclase, K-feldspar, quartz and muscovite (approximately 30–25 vol% plagioclase, 20–15 vol% K-feldspar, 40–35 vol% quartz, 10–5 vol% muscovite) as well as titanite and tourmaline as accessory phases.

## Whole-rock major, trace and rare earth elements

Major, trace and rare earth element (REE) compositions of forty-eight metagranitoids (including granitic, leucogranitic and pegmatitic dikes) are listed in supplementary Tables S2a-c and plotted in Figs. 5, 6, 7, 8, 9 and 10. Selected typical analytical data on major, trace and rare earth element (REE) compositions for the distinct plutonic suites are provided in Table 1. Major element data from twenty-eight samples from Mandl et al. (2018) (MM1, MM2, MM10, MM12, MM13, MM14, MM15, MM17, MM18, MM19, MM20, MM22, MM23, MM27, MM28, MM32, MM33, MM54, MM55, MM56, MM57, MM65, MM66), and Pfingstl et al. (2015) (SP54, SP58, SP78, SP79, SP81) as well as radiogenic Rb and Sr isotope data from eight samples (Pfingstl et al. 2015) (supplementary Table S2) were also included, as these are part of the complete data set discussed in this study. All metagranitoids of the Seckau Complex follow the calc-alkaline fractionation trend (Irvine and Baragar 1971) and in the Peccerillo and Taylor (1976) diagram the calc-alkaline to high K calc-alkaline series. Metagranitoid rocks of the Hochreichart Plutonic Suite (HrPS) predominantly fall in the granite field, whereas metagranitoids of the Hintertal Plutonic Suite (HtPS), subdivided into the Pletzen Pluton (PltzP) and the Griessstein Pluton (GrstP), range in their composition from quartz monzodiorite to granodiorite to granite (Fig. 5a).

Granites of the Hochreichart Plutonic Suite show a consistently peraluminous character (Shand 1943) and reflect S-type to minor I-type affinity (Chappell and White 2001) with A/CNK values (molar proportions of $Al_2O_3$/ ($CaO + Na_2O + K_2O$)) in the range between 1.08 and 1.51 and A/NK values (molar proportions of $Al_2O_3$/ ($Na_2O + K_2O$)) ranging from 1.15 to 1.73.

Metagranitoids of the Hintertal Plutonic Suite show a meta- to peraluminous trend for the Pletzen Pluton and peraluminous character for the Griessstein Pluton, with A/CNK values ranging from 0.88 to 1.10 and 1.10 to 1.23 for the Pletzen and Griesstein Pluton, respectively. The A/NK values for the Pletzen Pluton range from 1.43 to 2.31, and from 1.34 to 1.58 for the Griessstein Pluton (Fig. 5b).

On the (Y + Nb) vs. Rb tectonic discrimination diagram for granites (Pearce et al. 1984) the metagranitoids of the Hochreichart Plutonic Suite and the Hintertal Plutonic Suite plot predominantly in the volcanic-arc granite field (VAG), reflecting geochemical signatures of an active continental margin. Only few samples are marginally located in the syn-collisional granites field (syn-COLG; MM63, MM36) and in the within-plate granite field (WPG; MM33, SP79, MM32, SP59), respectively (Fig. 6). However, most likely, these samples also reflect a VAG setting.

### Hochreichart plutonic suite

Binary major oxide vs. $SiO_2$ variation diagrams for peraluminous metagranitoids of the Hochreichart Plutonic Suite show typical fractionation trends for most of the major oxides. There is a general decrease in $TiO_2$, $Al_2O_3$, MgO, CaO (Fig. 7a-d), $P_2O_5$, FeOt and MnO with increasing $SiO_2$,(Fig. 7g-i), whereas $Na_2O$ and $K_2O$ (Fig. 7e,f) indicate no significant fractionation trend. The metagranitoids generally show high contents of $SiO_2$ (67.77–77.84 wt%), $Na_2O$ (1.84–5.08 wt%) and $K_2O$ (1.50–5.43 wt%). Their $TiO_2$ values vary from 0.06 to 0.60 wt%, $Al_2O_3$ ranges from 12.28–16.22 wt%, $Fe_2O_3$ (total Fe) content is between 1.02 to 4.69 wt% and MnO values are in the range between 0.02–0.06 wt%. MgO values vary between 0.12 and 1.80 wt% and CaO and $P_2O_5$ contents range from 0.21 to 2.05 wt% and from 0.04 to 0.17 wt%, respectively. Large ion lithophile elements (LIL), e.g., Rb, Ba (Fig. 8a, c) and transition metals such as Sc, V and Cr (Fig. 8d-f), predominantly display a negative correlation with $SiO_2$, whereas high field strength elements (HFSE e.g., Y, Zr, Nb) (Fig. 8g-i) show no significant fractionation trend or display only a slight decrease against $SiO_2$. Rb values are usually high and range between 91 and 229 µg/g, with the exception for samples MM13 (32 µg/g) and MM27 (64 µg/g), Sr contents are low with an average of about 100 µg/g, and Ba values vary from 186 to 956 µg/g. Sc contents are between 2 and 12 µg/g, V values ranges from 2 to 66 µg/g, and Cr contents vary between 1 and 35 µg/g. Y and Zr values range from 5 to 58 µg/g and 40 to 262 µg/g, respectively; Nb contents range from 4 to 17 µg/g (Table 1; supplementary Table S2a).

On the mantle-normalized (McDonough and Sun 1995) multi-element variation diagram, the metagranitoids of the Hochreichart Plutonic Suite show consistent trace element patterns, with enrichment in Rb, U, K, Pb, Nd, Sm and strong depletion in Ba, Nb, Ta, Sr, P and Ti as well as relatively flat distribution patterns in HREE (Fig. 9a). On the chondrite-normalized (McDonough and Sun 1995) REE diagram these rocks display an enrichment in LREE relative to HREE with $(La/Yb)_N$ of 2.23- 25.06 [$(La/Sm)_N = 1.95–4.01$; $(Dy/Yb)_N = 0.8–1.73$], and moderate negative Eu anomalies with $(Eu/Eu^*)_N$ values of 0.15- 0.77 (calculated after Taylor and

**Table 1** Selected whole-rock major (wt%), trace element and REE compositions (µg/g) for metagranitoids of the Hochreichart and Hintertal Plutonic Suites; *major elements, Rb and Sr analytical data published in Mandl et al. (2018); published data are displayed in *italic* notation. Sample MM16 is a reference sample for the chemical composition of paragneisses that were used for rhyolite-MELTS calculations (Gualda et al. 2012)

| | Hochreichart Plutonic Suite | | | | | | | Pletzen Pluton | | | | | Griessstein Pluton | | | Dikes | | | | Paragn |
|---|---|---|---|---|---|---|---|---|---|---|---|---|---|---|---|---|---|---|---|---|
| **sample** | **MM36** | **MM59** | **MM60** | **MM62** | **MM64** | **MM68** | **SP62** | **MM17*** | **MM23*** | **MM55*** | **MM65*** | **SP59** | **MM21** | **MM52** | **SP53** | **MM3** | **MM51** | **MM69** | **SP61** | **MM16** |
| ***major element oxide contents in weight percent (wt%)*** | | | | | | | | | | | | | | | | | | | | |
| $SiO_2$ | 74.90 | 70.12 | 72.60 | 71.10 | 73.90 | 75.28 | 69.22 | *68.41* | *67.73* | *63.08* | *62.73* | 59.14 | 73.07 | 70.40 | 70.30 | 75.31 | 75.56 | 75.82 | 74.92 | 67.26 |
| $TiO_2$ | 0.20 | 0.31 | 0.17 | 0.24 | 0.20 | 0.06 | 0.45 | *0.63* | *0.53* | *0.70* | *0.72* | 1.01 | 0.28 | 0.37 | 0.38 | 0.04 | 0.06 | 0.07 | 0.08 | 0.69 |
| $Al_2O_3$ | 13.22 | 14.61 | 14.23 | 15.09 | 14.09 | 13.62 | 15.31 | *15.06* | *15.61* | *16.94* | *16.77* | 17.06 | 14.27 | 14.49 | 14.83 | 13.92 | 13.97 | 12.93 | 14.23 | 15.13 |
| $Fe_2O_3$ | 1.88 | 2.43 | 1.43 | 2.36 | 1.15 | 1.02 | 3.24 | *3.53* | *3.34* | *4.53* | *4.73* | 6.47 | 1.93 | 2.51 | 2.40 | 0.44 | 0.60 | 0.56 | 1.00 | 5.59 |
| MnO | 0.030 | 0.052 | 0.021 | 0.041 | 0.021 | 0.032 | 0.058 | *0.070* | *0.063* | *0.074* | *0.079* | 0.127 | 0.048 | 0.038 | 0.038 | 0.038 | 0.026 | 0.014 | 0.025 | 0.11 |
| MgO | 0.47 | 0.85 | 0.39 | 0.55 | 0.31 | 0.12 | 0.97 | *1.41* | *1.29* | *1.80* | *1.86* | 2.58 | 0.56 | 1.24 | 0.98 | 0.08 | 0.09 | 0.13 | 0.33 | 2.32 |
| CaO | 0.32 | 1.60 | 0.70 | 1.31 | 0.21 | 0.27 | 1.69 | *1.75* | *2.67* | *4.30* | *4.22* | 4.89 | 1.13 | 0.95 | 1.24 | 0.77 | 0.49 | 0.41 | 1.65 | 2.37 |
| $Na_2O$ | 1.84 | 3.75 | 5.08 | 4.33 | 3.07 | 3.49 | 3.55 | *3.82* | *4.19* | *4.27* | *4.13* | 3.58 | 3.96 | 3.77 | 4.14 | 2.84 | 3.85 | 2.98 | 4.42 | 4.06 |
| $K_2O$ | 5.43 | 3.87 | 3.04 | 2.99 | 4.96 | 4.62 | 3.44 | *3.95* | *2.98* | *2.47* | *2.56* | 2.45 | 3.79 | 3.76 | 2.86 | 5.85 | 4.62 | 5.73 | 1.26 | 1.18 |
| $P_2O_5$ | 0.112 | 0.158 | 0.076 | 0.101 | 0.126 | 0.072 | 0.092 | *0.180* | *0.183* | *0.258* | *0.269* | 0.321 | 0.099 | 0.133 | 0.166 | 0.097 | 0.109 | 0.098 | 0.107 | 0.15 |
| LOI | 1.31 | 1.22 | 1.13 | 0.96 | 0.94 | 0.72 | 0.73 | 0.95 | 0.85 | 0.57 | 0.66 | *1.13* | 0.67 | 1.54 | 1.61 | 0.39 | 0.45 | 0.36 | 0.80 | 1.12 |
| analytical sum | 99.71 | 98.97 | 98.88 | 99.07 | 98.97 | 99.30 | 98.94 | 99.76 | 99.43 | 98.99 | 98.73 | 99.02 | 99.81 | 99.21 | 99.09 | 99.78 | 99.81 | 99.09 | 98.82 | 99.96 |
| ***trace element contents in parts per million (ppm; µg/g)*** | | | | | | | | | | | | | | | | | | | | |
| Li | 17.0 | 46.0 | 32.7 | 43.7 | 15.2 | 7.5 | 37.8 | 30.0 | 33.4 | 31.2 | 38.7 | 94.7 | 34.9 | 27.7 | 31.8 | 5.67 | 9.70 | 7.77 | 7.22 | 25.31 |
| Sc | 3.78 | 4.37 | 3.66 | 5.66 | 2.44 | 3.03 | 5.79 | 9.24 | 6.69 | 9.74 | 7.47 | 23.6 | 4.78 | 4.63 | 2.42 | 2.45 | 2.81 | 2.35 | 2.04 | 12.03 |
| V | 12.4 | 28.7 | 11.3 | 19.3 | 9.7 | 2.5 | 41.1 | 55.8 | 53.2 | 77.8 | 77.7 | 137 | 19.9 | 34.9 | 29.6 | 1.67 | 2.35 | 3.24 | 7.85 | 66.54 |
| Cr | 4.36 | 4.97 | 2.74 | 2.89 | 4.20 | 1.46 | 24.9 | 12.3 | 11.8 | 16.1 | 16.1 | 7.81 | 4.03 | 12.9 | 5.46 | 1.33 | 1.93 | 1.74 | 7.98 | 49.18 |
| Co | 32.8 | 30.0 | 52.1 | 29.8 | 37.0 | 38.6 | 48.2 | 33.1 | 42.7 | 38.6 | 31.3 | 30.1 | 40.7 | 19.2 | 3.07 | 42.3 | 41.1 | 36.3 | 50.1 | 21.27 |
| Ni | 3.04 | 1.71 | 1.10 | 1.20 | 1.32 | 0.58 | 10.3 | 4.70 | 4.28 | 5.52 | 5.58 | 5.52 | 1.54 | 2.51 | 2.11 | 1.39 | 0.82 | 1.12 | 3.89 | 11.70 |
| Cu | 4.75 | 3.23 | 10.8 | 4.19 | 0.53 | 0.52 | 6.65 | 2.37 | 4.09 | 4.89 | 5.96 | 8.66 | 3.00 | 0.79 | 1.23 | 1.63 | 0.40 | 3.51 | 7.37 | 19.34 |
| Zn | 0.13 | 0.66 | 0.32 | 0.64 | 0.09 | 0.28 | 52.5 | 59.7 | 67.3 | 0.97 | 0.91 | 108 | 0.52 | 0.31 | 23.7 | 8.87 | 18.7 | 0.23 | 12.7 | 55.53 |
| Ga | 20.3 | 20.0 | 19.8 | 23.8 | 22.5 | 21.6 | 17.9 | 19.5 | 18.5 | 23.4 | 22.2 | 20.5 | 19.8 | 18.6 | 17.3 | 14.9 | 16.8 | 14.8 | 14.6 | 9.29 |
| Rb | 192 | 156 | 117 | 159 | 229 | 192 | 123 | *104* | *78.5* | *69.0* | *73.8* | 76.7 | 118 | 95.3 | 107 | 122 | 115 | 135 | 30.7 | 32.00 |
| Sr | 31.5 | 241 | 74.9 | 116 | 57.0 | 58.0 | 128 | *416* | *534* | *756* | *733* | 522 | 247 | 166 | 164 | 114 | 53.9 | 94.3 | 267 | 321.00 |
| Y | 7.0 | 18.3 | 19.3 | 25.5 | 5.07 | 17.4 | 27.6 | 34.0 | 24.0 | 25.3 | 19.5 | 48.6 | 21.5 | 9.40 | 8.33 | 10.5 | 13.6 | 13.3 | 11.6 | 17.42 |
| Zr | 142 | 115 | 118 | 98.90 | 90.00 | 39.50 | 166 | 177 | 192 | 215 | 208 | 224 | 156 | 128 | 166 | 43.6 | 56.4 | 19.6 | 25.0 | 137.90 |
| Nb | 5.93 | 11.1 | 12.4 | 16.8 | 14.3 | 10.6 | 12.2 | 16.8 | 10.7 | 11.7 | 11.2 | 9.73 | 10.2 | 6.52 | 11.6 | 1.64 | 5.80 | 4.33 | 4.27 | 5.55 |
| Cs | 4.15 | 6.55 | 3.29 | 8.27 | 4.33 | 1.80 | 4.74 | 2.49 | 2.54 | 2.04 | 1.81 | 6.36 | 3.52 | 4.91 | 3.27 | 4.23 | 1.57 | 2.50 | 0.44 | 1.19 |
| Ba | 298 | 682 | 410 | 261 | 501 | 365 | 555 | 868 | 1122 | 1015 | 1085 | 1078 | 1065 | 983 | 617 | 699 | 377 | 404 | 183 | 350.59 |
| Ta | 1.40 | 1.80 | 2.44 | 2.45 | 3.21 | 2.32 | 2.10 | 1.83 | 1.64 | 1.54 | 1.38 | 1.02 | 1.49 | 0.63 | 1.03 | 1.18 | 1.36 | 1.39 | 2.10 | 0.68 |
| Pb | 4.91 | 18.2 | 18.5 | 12.3 | 10.5 | 25.0 | 12.1 | 19.6 | 16.1 | 17.7 | 15.4 | 16.8 | 35.9 | 10.2 | 4.11 | 23.9 | 26.6 | 41.2 | 11.2 | 13.32 |

**Table 1** (continued)

| Hochreichart Plutonic Suite | | | | | | | | Pletzen Pluton | | | | | Griessstein Pluton | | | Dikes | | | | Paragn |
|---|---|---|---|---|---|---|---|---|---|---|---|---|---|---|---|---|---|---|---|---|
| **sample** | **MM36** | **MM59** | **MM60** | **MM62** | **MM64** | **MM68** | **SP62** | **MM17*** | **MM23*** | **MM55*** | **MM65*** | **SP59** | **MM21** | **MM52** | **SP53** | **MM3** | **MM51** | **MM69** | **SP61** | **MM16** |
| Th | 3.32 | 9.98 | 10.3 | 12.3 | 10.3 | 7.48 | 9.16 | 19.2 | 8.66 | 9.30 | 6.69 | 18.6 | 14.3 | 6.52 | 6.04 | 1.47 | 4.67 | 2.98 | 4.97 | 4.55 |
| U | 0.57 | 5.99 | 2.93 | 5.45 | 3.47 | 2.55 | 2.72 | 4.75 | 2.37 | 2.26 | 2.28 | 2.65 | 2.75 | 0.97 | 1.54 | 1.83 | 4.06 | 2.58 | 5.81 | 1.07 |
| ***rare-earth element (REE) contents in parts per million (ppm; µg/g)*** | | | | | | | | | | | | | | | | | | | | |
| La | 9.31 | 22.01 | 20.04 | 19.14 | 15.84 | 9.29 | 17.78 | 93.95 | 38.93 | 38.25 | 25.77 | 97.71 | 24.63 | 22.88 | 17.04 | 3.66 | 7.08 | 4.14 | 3.93 | 16.27 |
| Ce | 27.27 | 61.38 | 47.78 | 48.49 | 52.86 | 20.49 | 44.86 | 163.15 | 73.10 | 103.63 | 97.24 | 136.47 | 60.77 | 53.41 | 53.23 | 4.40 | 12.72 | 9.69 | 7.47 | 27.97 |
| Pr | 2.81 | 5.62 | 4.89 | 5.12 | 3.92 | 2.44 | 4.93 | 16.35 | 8.01 | 10.09 | 7.32 | 21.46 | 5.94 | 5.28 | 3.82 | 0.79 | 1.70 | 1.10 | 1.21 | 4.22 |
| Nd | 11.36 | 21.86 | 18.88 | 19.65 | 14.60 | 9.04 | 20.76 | 59.56 | 31.98 | 39.47 | 29.73 | 87.21 | 22.50 | 19.62 | 15.07 | 3.18 | 6.67 | 4.22 | 4.72 | 17.48 |
| Sm | 2.27 | 4.44 | 4.33 | 4.68 | 2.81 | 2.43 | 5.01 | 10.65 | 6.59 | 7.30 | 5.67 | 17.07 | 4.73 | 3.32 | 2.66 | 0.78 | 1.87 | 1.32 | 0.99 | 3.78 |
| Eu | 0.35 | 0.89 | 0.57 | 0.61 | 0.22 | 0.22 | 0.65 | 1.73 | 1.49 | 1.75 | 1.41 | 3.34 | 0.90 | 0.94 | 0.45 | 0.67 | 0.29 | 0.40 | 0.17 | 0.89 |
| Gd | 1.72 | 4.02 | 3.96 | 4.72 | 2.09 | 2.44 | 3.00 | 6.18 | 3.81 | 6.42 | 5.03 | 9.32 | 4.44 | 2.76 | 1.53 | 0.60 | 1.23 | 1.58 | 0.61 | 2.27 |
| Tb | 0.26 | 0.57 | 0.59 | 0.79 | 0.23 | 0.45 | 0.57 | 0.86 | 0.58 | 0.85 | 0.68 | 1.38 | 0.65 | 0.33 | 0.22 | 0.15 | 0.27 | 0.33 | 0.16 | 0.39 |
| Dy | 1.52 | 3.33 | 3.50 | 4.66 | 1.07 | 2.97 | 4.40 | 5.92 | 4.30 | 4.71 | 3.77 | 9.15 | 3.87 | 1.76 | 1.50 | 1.48 | 2.32 | 2.32 | 1.69 | 3.00 |
| Ho | 0.30 | 0.63 | 0.66 | 0.88 | 0.18 | 0.59 | 0.88 | 1.06 | 0.79 | 0.92 | 0.73 | 1.64 | 0.75 | 0.34 | 0.29 | 0.33 | 0.42 | 0.46 | 0.35 | 0.59 |
| Er | 0.85 | 1.70 | 1.78 | 2.30 | 0.46 | 1.67 | 1.92 | 2.38 | 1.69 | 2.44 | 1.93 | 3.35 | 1.89 | 0.82 | 0.59 | 0.80 | 0.95 | 1.26 | 0.94 | 1.35 |
| Tm | 0.12 | 0.22 | 0.24 | 0.31 | 0.06 | 0.24 | 0.34 | 0.45 | 0.31 | 0.31 | 0.25 | 0.53 | 0.23 | 0.10 | 0.11 | 0.19 | 0.20 | 0.18 | 0.22 | 0.25 |
| Yb | 0.91 | 1.61 | 1.69 | 2.20 | 0.43 | 1.83 | 2.24 | 2.76 | 1.90 | 2.08 | 1.67 | 3.33 | 1.50 | 0.68 | 0.80 | 1.38 | 1.37 | 1.30 | 1.77 | 1.56 |
| Lu | 0.14 | 0.25 | 0.25 | 0.35 | 0.07 | 0.27 | 0.31 | 0.45 | 0.29 | 0.31 | 0.25 | 0.49 | 0.24 | 0.10 | 0.11 | 0.24 | 0.22 | 0.19 | 0.29 | 0.25 |
| ***calculated element ratios*** | | | | | | | | | | | | | | | | | | | | |
| A/CNK | 1.40 | 1.10 | 1.10 | 1.18 | 1.31 | 1.21 | 1.21 | 1.10 | 1.04 | 0.97 | 0.97 | 0.98 | 1.13 | 1.21 | 1.22 | 1.12 | 1.14 | 1.09 | 1.22 | |
| A/NK | 1.49 | 1.41 | 1.22 | 1.46 | 1.35 | 1.27 | 1.60 | 1.43 | 1.54 | 1.75 | 1.75 | 2.00 | 1.34 | 1.41 | 1.50 | 1.26 | 1.23 | 1.16 | 1.65 | |
| $(Eu/Eu^*)_N$ | 0.55 | 0.64 | 0.42 | 0.40 | 0.27 | 0.28 | 0.51 | 0.65 | 0.91 | 0.78 | 0.81 | 0.81 | 0.60 | 0.95 | 0.68 | 2.98 | 0.57 | 0.85 | 0.68 | |
| $(La/Yb)_N$ | 6.92 | 9.27 | 8.07 | 5.91 | 25.06 | 3.45 | 5.39 | 23.11 | 13.89 | 12.49 | 10.51 | 19.95 | 11.12 | 22.86 | 14.47 | 1.80 | 3.52 | 2.17 | 1.51 | |

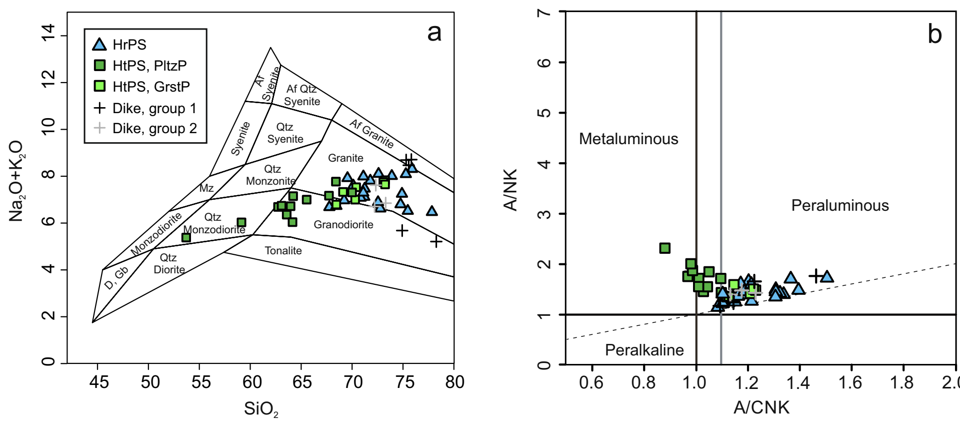


**Fig. 5** (**a**) TAS (total alkali vs. silica; wt%) classification diagram (Middlemost 1994) and (**b**) A/NK vs. A/CNK plot (Shand 1943) for metagranitoids (including granitic-, leucogranitic- and pegmatitic dikes) of the Hochreichart Plutonic Suite (HrPS) and the Hintertal Plutonic Suite (HtPS) comprising the Pletzen Pluton (PltzP) and the Griesstein Pluton (GrstP). In Fig. 5b the division between metaluminous and peraluminous granites is at A/CNK 1.0 (Shand 1943), the division between I-type and S-type granites is at A/CNK 1.1 (Chappel and White 2001)

McLennan 1985; $(Eu/Eu^*)_N = Eu_N/\sqrt{(Sm_N{}^*Gd_N)}$) (Fig. 9b). A slightly negative Ce anomaly can only be observed in sample MM32.

## Hintertal plutonic suite

Meta- to peraluminous metagranitoids of the Hintertal Plutonic Suite show similar fractionation trends compared to the Hochreichart Plutonic Suite for most major oxides (Fig. 7), but display a larger variation in $SiO_2$ and have a positive correlation of $K_2O$ with $SiO_2$ (Fig. 7f). However, trace element variation diagrams (Fig. 8) show clear differences in their distribution pattern of predominantly LIL elements. Rb indicates a positive correlation with $SiO_2$ (Fig. 8a), Sr a negative one (Fig. 8b), and Ba content is more or less constant with an average of about 1060 µg/g (Fig. 8c). Sc, V, Cr, Y and Zr indicate negative trends (Fig. 8d-h). Nb is more or less constant with an average of about 12 µg/g at $SiO_2$ values < 70 wt% and decreases then with increasing $SiO_2$ (Fig. 8i).

Based on field observations, petrographic, geochemical and geochronological criteria, the metagranitoids of the Hintertal Plutonic Suite can be subdivided into (a) the Pletzen Pluton and (b) the Griessstein Pluton (Mandl et al. 2018). Consequently, metagranitoids of the Hintertal Plutonic Suite are discussed separately with regard to the aforementioned plutons.

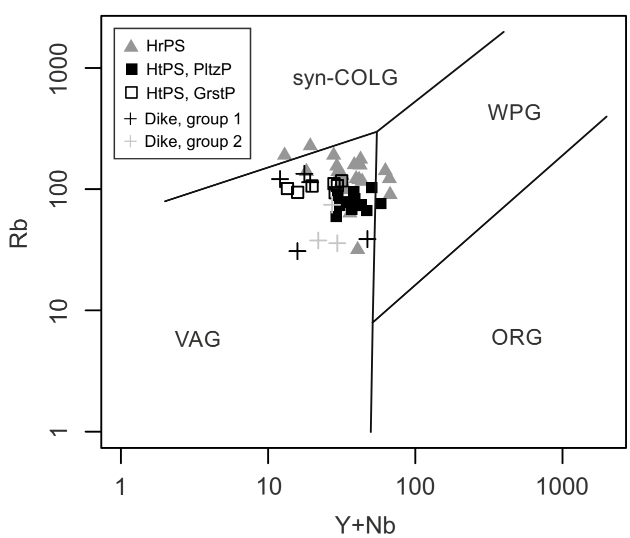


**Fig. 6** Geotectonic discrimination diagram (Rb vs. (Y + Nb); µg/g) for granitoids rocks (Pearce et al. 1984) of the Seckau Complex showing the fields of volcanic-arc granites (VAG), syn-collisional granites (syn-COLG), within-plate granites (WPG) and ocean-ridge granites (ORG). Abbreviations: HrPS: Hochreichart Plutonic Suite, HtPS: Hintertal Plutonic Suite, comprising the Pletzen Pluton (PltzP) and the Griesstein Pluton (GrstP)

## Pletzen pluton of the hintertal plutonic suite

The intermediate to acidic rocks of the Pletzen Pluton show a meta- to peraluminous character and display low A/CNK contents ranging from 0.88 to 1.10 compared to the Griessstein Pluton (Fig. 5b). On binary variation diagrams of major oxides and trace elements versus $SiO_2$ (Figs. 7 and 8) these samples display the highest contents in $TiO_2$ (0.43–1.03 wt%), $Al_2O_3$ (14.56–17.54 wt%), MgO (1.03–4.51 wt%), CaO (1.75–6.80 wt%), $P_2O_5$ (0.15–0.39 wt%), $Fe_2O_3$ (3.03–9.04 wt%), MnO (0.06–0.18 wt%), Sr (416–762 µg/g), Sc (7–24 µg/g), V (48–214 µg/g) Y (18–49 µg/g) and Zr (165–308 µg/g) as well as the lowest contents in $SiO_2$ (53.71–70.00 wt%), $K_2O$ (2.22–3.95 wt%)

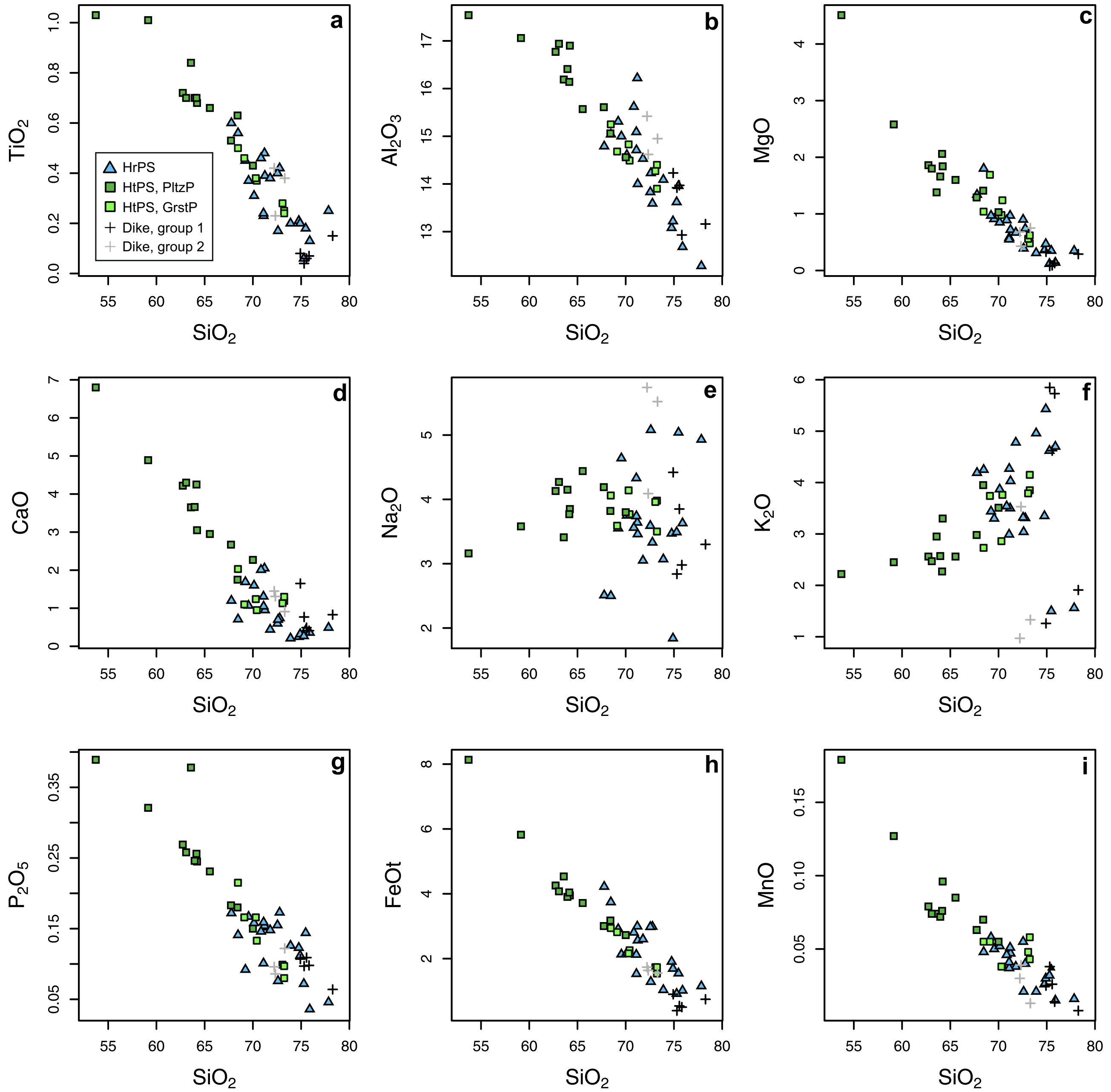


**Fig. 7** Major elements (wt%) vs. $SiO_2$ (wt%) variation diagrams for metagranitoids of the Seckau Complex. Abbreviations:HrPS: Hochreichart Plutonic Suite, HtPS: Hintertal Plutonic Suite, PltzP: Pletzen Pluton, GrstP: Griessstein Pluton

and Rb (60–104 µg/g) of all analyzed samples from the Hintertal Plutonic Suite. $Na_2O$ values are high and range between 3.16 and 4.44 wt%. Barium and Nb are nearly constant with a mean of 1058 µg/g and 12 µg/g, respectively (Table 1; supplementary Table S2b). On the mantle-normalized (McDonough and Sun 1995) multi-element variation diagram, negative Nb, Ta, P, and Ti anomalies are observed (Fig. 9c). In the chondrite-normalized (McDonough and Sun 1995) REE distribution diagram (Fig. 9d) the metagranitoids are enriched in LREE relative to HREE with $(La/Yb)_N$ ratios of 8.68 to 28.84 [$(La/Sm)_N$ = 2.38–5.51; $(Dy/Yb)_N$ = 1.27–1.97] and are characterized by the absence of a significant Eu anomaly with $(Eu/Eu^*)_N$ values in the range between 0.65 and 0.95.

## Griessstein pluton of the hintertal plutonic suite

Metagranitoids of the Griessstein Pluton have a consistently peraluminous character (A/CNK = 1.10–1.23) (Fig. 5b). Major oxides of the Griessstein Pluton usually have the

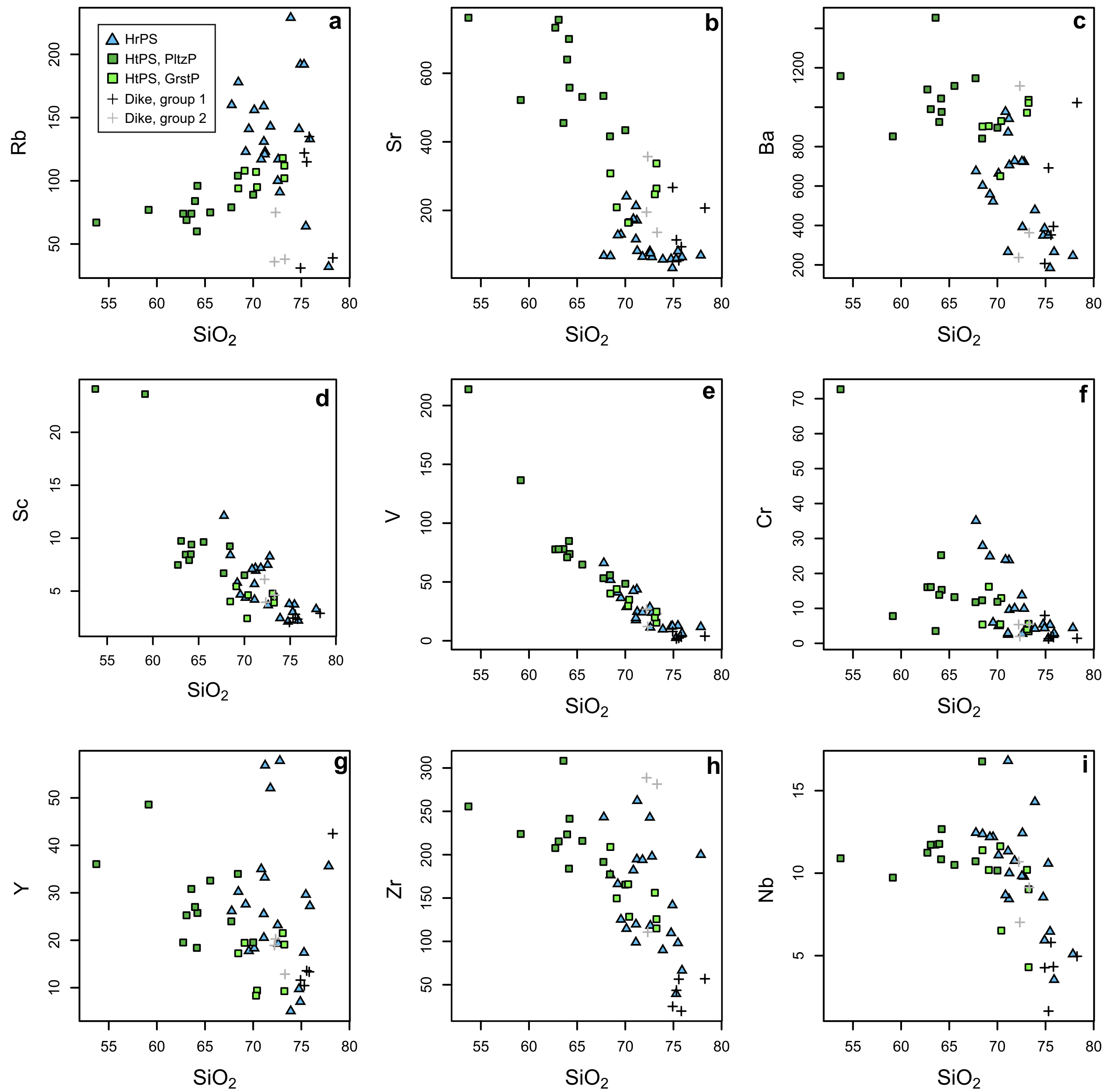


**Fig. 8** Selected trace elements (µg/g) vs. $SiO_2$ (wt%) variation diagrams for metagranitoids of the Seckau Complex. Abbreviations: HrPS: Hochreichart Plutonic Suite, HtPS: Hintertal Plutonic Suite, PltzP: Pletzen Pluton, GrstP: Griessstein Pluton

lowest $TiO_2$, $Al_2O_3$, MgO, CaO, $P_2O_5$, FeOt and MnO (Fig. 7a-d, g-i) values and the highest $K_2O$ (Fig. 7f) contents for all samples of the Hintertal Plutonic Suite. They are characterized by moderate to high concentrations of $SiO_2$ (64.48–73.24 wt %), $Na_2O$ (3.50–4.14 wt%) and $K_2O$ (2.73–4.15 wt%). Their $TiO_2$ content ranges from 0.24 to 0.50 wt%, $Al_2O_3$ values range from 13.90 to 15.25 wt%, $Fe_2O_3$ contents are between 1.71 and 3.27 wt%, MnO is between 0.04 and 0.06 wt%, MgO varies from 0.48 to 1.69 wt%, CaO from 0.95 to 2.03 wt% and $P_2O_5$ values range from 0.08 to 0.22 wt%. Metagranitoids of the Griessstein Pluton display the highest Rb values (94–118 µg/g) and the lowest Sr (164–337), Sc (2–5 µg/g) V (15–44 µg/g), Cr (3–16 µg/g), Y (8–22 µg/g) and Zr (115–209 µg/g) values (Figs. 7 and 8, Table 1; supplementary Table S2b). On the mantle-normalized multi-element diagram (Fig. 9e) after McDonough and Sun (1995) the Griessstein Pluton displays strong negative Nb, Ta, P, and Ti anomalies as well as a positive K and Pb anomaly. The chondrite-normalized REE distribution patterns (McDonough and Sun 1995)

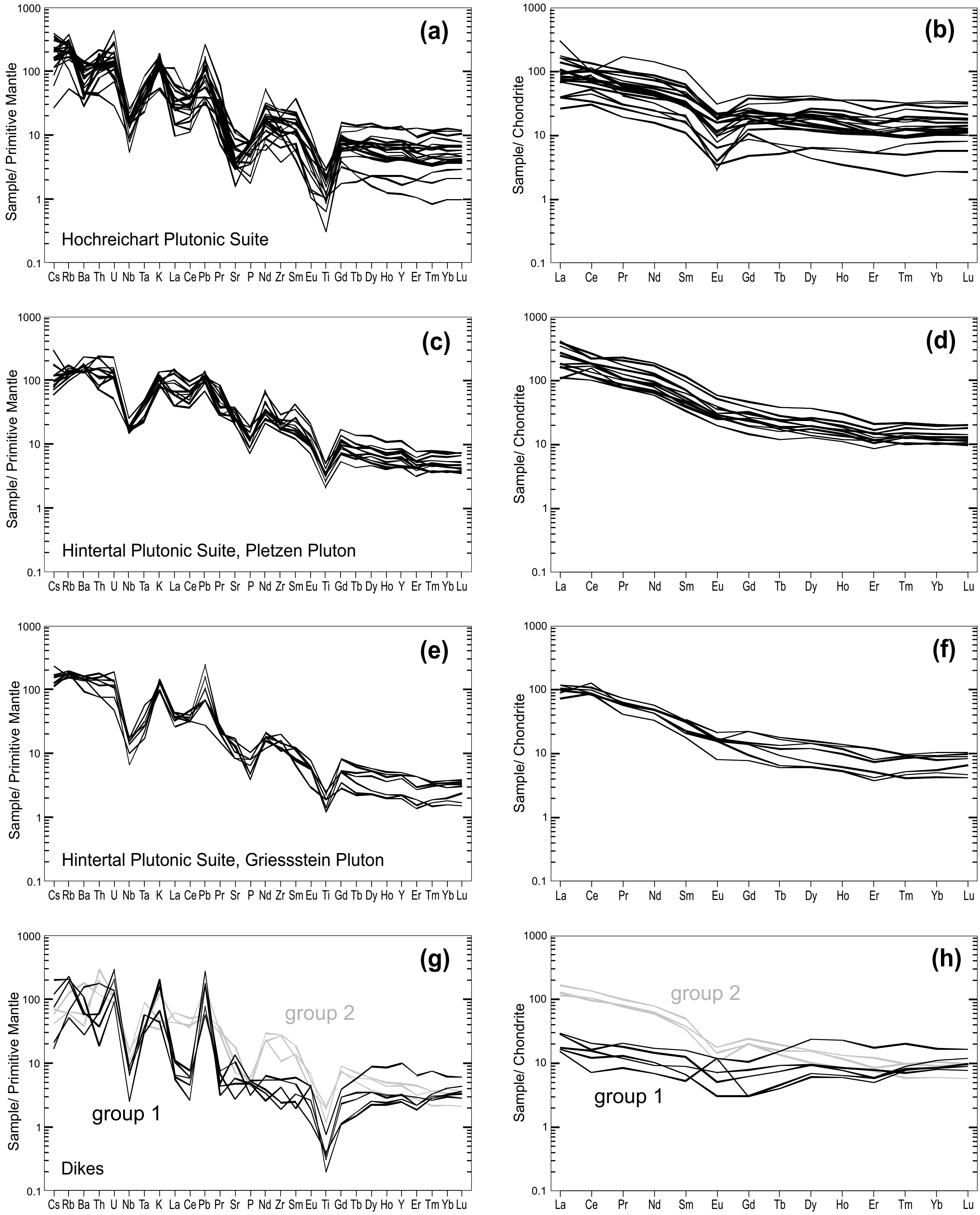


**Fig. 9** Primitive mantle normalized trace element (μg/g) distribution patterns and chondrite-normalized REE patterns for metagranitoids of the Seckau Complex (normalization values after (McDonough and Sun 1995): (**a**, **b**) for the metagranitoids of the Hochreichart Plutonic Suite, (**c**, **d**) for metagranitoids of the Pletzen Pluton of the Hintertal Plutonic Suite, (**e**, f) for metagranitoids of the Griessstein Pluton of the Hintertal Plutonic Suite and (**g**, **h**) for leucogranitic- and granitic dikes

from metagranitoids of the Griessstein Pluton are similar to the Pletzen Plutonic Suite, but slightly less enriched in REEs. The $(La/Yb)_N$ ratio varies between 9.95 and 22.86 [$(La/Sm)_N = 2.87–5.63$; $(Dy/Yb)_N = 1.14–1.80$]. A minor negative Eu anomaly with an average of $(Eu/Eu^*)_N = 0.81$ is developed (Fig. 9f).

### Dikes

Granitic, leucogranitic and pegmatitic dikes vary widely in their major and trace element composition (Table 1; supplementary Table S2c). Partly they define a separate trend as seen in the $SiO_2$ vs $K_2O$ and $SiO_2$ vs Rb bivariate diagrams (Figs. 7 and 8). On mantle-normalized and chondrite-normalized multi-element variation diagrams (McDonough and Sun 1995) the dikes fall into two distinct groups.

The first group contains pegmatitic dikes intruding the paragneisses (Glaneck Metamorphic Suite) (MM5, MM51, SP61). Further, one leucogranitic dike (MM3) and one granitic dike (MM69) intruded into the metagranitoids of the Hochreichart Plutonic Suite. The samples are dominated by positive Rb, U, K and Pb anomalies as well as negative Nb and Ti anomalies (Fig. 9g). On the chondrite-normalized (McDonough and Sun 1995) REE diagram (Fig. 9h), LREE and HREE patterns are relative constant with $(La/Yb)_N$ ranging from 1.51 to 3.52. A negative Eu anomaly with $(Eu/Eu^*)_N$ values vary from and 0.57 to 0.92, with the exception of sample MM3, which has a positive Eu anomaly.

The second group comprises fine-grained, small-sized concordant granitic dikes (MM14, MM15, MM54) that intruded into the paragneisses (Glaneck Metamorphic Suite). This group is characterized by a negative Nb, P and Ti anomaly (Fig. 9g), an enrichment in LREE relative to HREE with $(La/Yb)_N$ of 12.35–19.72, and a negative Eu anomaly with $(Eu/Eu^*)_N = 0.39–0.59$ (Fig. 9h, Table 1; supplementary Table S2c). Very close to this site, a huge granitic intrusive body, being part of the Hochreichart Plutonic Suite, (sample MM13), also penetrates the paragneiss.

## Discussion

### Geochemical evolution of the magmatic suites of the Seckau Complex

The granitoids of the Seckau Complex were previously considered to be part of the intra-Alpine Variscan intrusive complexes (e.g., Schermaier et al. 1997). New geochronological data, however, revealed that the metagranitoids of the Seckau Complex are part of both Late Cambrian to Early Ordovician, and Late Devonian to Mississippian (i.e. early Variscan) plutons (Mandl et al. 2018). This requires, therefore, a re-evaluation of the pre-Alpine evolution of this part of the Eastern Alps, and its magmatic and geochemical development in particular, as the distinct plutonic suites need to be treated separately in terms of crystallization and fractionation trends. Both intrusive complexes, however, display geochemical characteristics of volcanic-arc granites and are therefore related to distinct active continental margins.

### Hochreichart plutonic suite

Metagranitoids of the Hochreichart Plutonic Suite are chemically evolved and, calculated back to the time of emplacement (~496 Ma), display relatively low initial $^{87}Sr/^{86}Sr$ values between 0.7056 and 0.7061 (Table 2) displaying I- and S- type geochemical characteristics. These metagranitoids show generally high Rb values and a low Sr content resulting in a high Rb/Sr ratio, being typical for an evolved granitic magma. Negative fractionation trends of several major and trace elements indicate the crystallization of zircon, apatite, Fe-Ti-oxide, feldspar and subordinately of biotite with cooling. The presence of a negative Eu anomaly, seen in chondrite-normalized multi-element variation diagrams (Fig. 9b), indicates the crystallization and fractionation of plagioclase from the granitic source.

**Table 2** Calculated initial $^{87}Sr/^{86}$ Sr for metagranitoids of the Hochreichart Plutonic Suite (HrPS) and the Hintertal Plutonic Suite (Pletzen Pluton (HtPS, PltzP) and Griessstein Pluton (HtPS, GrstP)). Rb and Sr data (μg/g) were taken from Pfingstl et al. (2015) and the average age of the respective granitoids were calculated from U–Pb zircon ages represented in Mandl et al. (2018)

| Sample | Unit | Rb | Sr | Rb/Sr | $^{87}Rb/^{86}Sr$ | $(^{87}Sr/^{86}Sr)_{WR}$ | 2SE | $(^{87}Sr/^{86}Sr)_{353}$ | $(^{87}Sr/^{86}Sr)_{496}$ |
|---|---|---|---|---|---|---|---|---|---|
| SP62 | HrPS | 119 | 130 | 0.91 | 2.6421 | 0.724.216 | 0.000.004 | | 0.7056 |
| SP79 | HrPS | 122 | 86 | 1.42 | 4.1077 | 0.735.010 | 0.000.004 | | 0.7061 |
| SP58 | HtPS, PltzP | 73 | 470 | 0.16 | 0.4490 | 0.708.325 | 0.000.004 | 0.7061 | |
| SP59 | HtPS, PltzP | 75 | 540 | 0.14 | 0.4005 | 0.708.124 | 0.000.004 | 0.7061 | |
| SP80 | HtPS, PltzP | 75 | 550 | 0.14 | 0.3934 | 0.707.748 | 0.000.004 | 0.7058 | |
| SP81 | HtPS, PltzP | 90 | 647 | 0.14 | 0.4022 | 0.707.143 | 0.000.004 | 0.7051 | |
| SP53 | HtPS, GrstP | 108 | 168 | 0.64 | 1.8612 | 0.714.706 | 0.000.004 | 0.7054 | |
| SP54 | HtPS, GrstP | 91 | 318 | 0.29 | 0.8290 | 0.710.423 | 0.000.004 | 0.7063 | |

## Hintertal plutonic suite

The chemical fractionation of the Hintertal Plutonic Suite is clearly marked by major oxides and trace element trends vs. $SiO_2$ (Figs. 7 and 8). Most rocks of the fractionated Griessstein Pluton show similar decreasing $TiO_2$, $Al_2O_3$, MgO, CaO, $P_2O_5$, FeOt, MnO trends and increasing $K_2O$ values vs. $SiO_2$ but have lower or higher values compared to the more primitive Pletzen Pluton samples (Figs. 7, 8 and 10). Incompatible LIL elements such as Cs and Rb are enriched in the Griessstein Pluton compared to the Pletzen Pluton and Sr, HFS elements (e.g., Y, Zr, Ce) as well as transition metals (e.g., Sc, V, Cr, Ni) are enriched within the rocks of the Pletzen Pluton and indicate the crystallization of zircon, apatite, feldspar and biotite with cooling (Figs. 7, 8 and 10). Initial $^{87}Sr/^{86}Sr$ ratios from rocks of the Pletzen Pluton and the Griessstein Pluton calculated back to the time of emplacement (~353 Ma) vary between 0.7051—0.7061 and 0.7054 – 0.7063, respectively.

The similar geochemical behavior of K and Rb is also a good indicator to demonstrate fractionation effects on granitic melts (Cerńy et al. 1982; Quemeneur and Lagache 1999; London 2008). The correlation of e.g., K/Rb ratio vs. Sr (Fig. 10i) suggests that the studied granitoids of the Griesssstein Pluton are generally more evolved than the Pletzen Pluton granitoids and thus most likely have been derived from the same source. Interestingly, sample

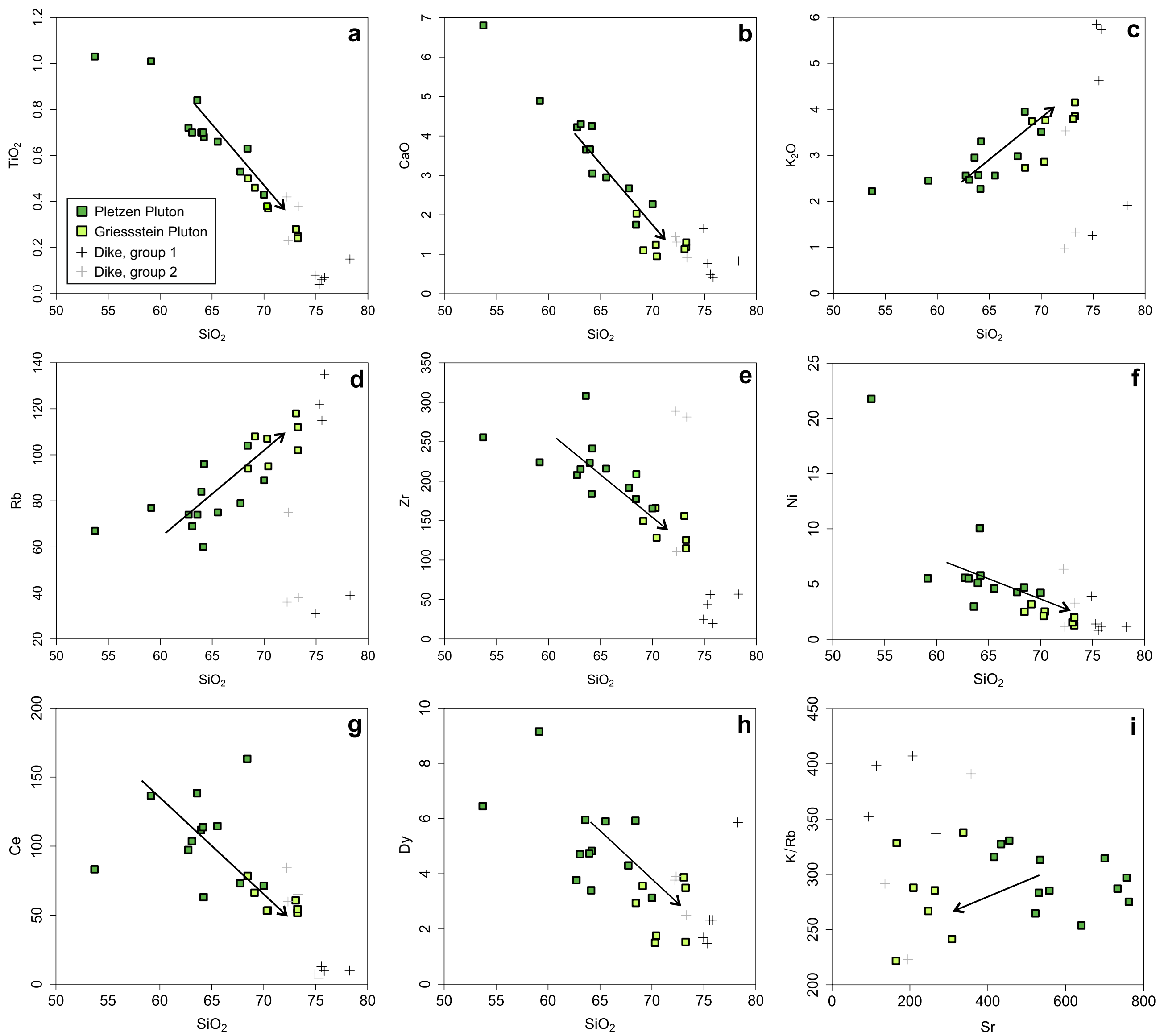


**Fig. 10** Element variation diagrams. (**a**-**h**) $SiO_2$ (wt%) vs major oxides (wt%) and trace elements (µg/g). (i) K/Rb ratio vs trace elements (µg/g) for metagranitoids of the Pletzen Pluton and the Griessstein Pluton as well as for pegmatitic and granitic dikes

MM22 deviates in this variation diagrams from the trend and might indicate slight wall rock contamination.

The spatial relationship of the different plutonic bodies, with small volumes of the Late Devonian/Early Carboniferous Griessstein Pluton occurring between the Late Devonian/Early Carboniferous Pletzen Pluton and the Late Cambrian/Early Ordovician Hochreichart Suite, points to two explanation models: (1) the Griessstein Pluton is the result of contamination of the Pletzen Pluton by the Hochreichart Suite wall rock or (2) the Griessstein Pluton represents a more evolved Pletzen Pluton composition. We therefore discuss the chemical characteristics of the different plutonic suites and use rhyolite-MELTS (Gualda et al. 2012) to compare observed compositions with calculated ones.

A possible assimilation of Hochreichart granitic rocks into the marginal portions of the Pletzen intrusives was tested in order to explain the differences between the two plutons of the Hintertal Suite. By using average major and trace element compositions of Hochreichart and Pletzen plutonic rocks it was not possible to obtain the measured composition of the Griessstein Pluton. Assuming an assimilation of 10% of the Hochreichart Pluton, lower $SiO_2$ and Rb values as well as higher Sr, V, Cr and Nd values would be required to reproduce the chemical composition of the Griessstein Pluton. Alternatively, we have also tested the Glaneck Metamorphic Suite paragneisses as contaminant for the Pletzen intrusives (representative chemical composition data of paragneisses are provided in Table 1; sample MM16, Fig. 3). Again, the observed chemical composition of the Griessstein Pluton could not be reproduced: by mixing 10% of paragneiss to the Pletzen Pluton; $SiO_2$, $TiO_2$, and $Al_2O_3$ remain constant, $K_2O$ and Rb decrease and MgO increases.

Therefore, we consider the Griessstein Pluton to be the product of a fractionation process from the Pletzen Pluton where probably only small amounts of wall rock or a $SiO_2$-rich melt were assimilated. Major element calculations derived from rhyolite-MELTS demonstrate that, at isobaric crystallization conditions of 0.3 GPa, 20 to 30% of the Pletzen melt (calculated with an average composition of the samples MM17, MM18, MM19, MM23, MM55, MM56, MM65) needs to crystallize in order to produce a composition close to the Griessstein Pluton (calculated with an average composition of the samples MM20, MM21, MM22, MM52, MM53, SP53) (Table 3). The more evolved nature of the Griessstein pluton is responsible for the peraluminous nature and stability of muscovite. The Sr isotopes are similar to the Pletzen Pluton. When considering the geochemistry of the Griessstein Pluton, then a I- to S- type character can be inferred, as the Sr isotopes display I-type, and the peralkaline affinity S-type characteristics. We conclude that the Griessstein Pluton is the result of 20 to 30% fractionation of mainly

**Table 3** Major element compositions used for calculation with rhyolite-MELTS (Gualda et al. 2012); compositions are composite values. Abbreviations: PltzP: Pletzen Pluton, GrstP: Griessstein Pluton

| | average PltzP composition [wt%] | average GrstP composition [wt%] | calculated 30% crystallized [wt%] |
|---|---|---|---|
| $SiO_2$ | 65.76 | 71.56 | 70.2 |
| $TiO_2$ | 0.63 | 0.33 | 0.72 |
| $Al_2O_3$ | 16.00 | 14.43 | 14.24 |
| $Fe_2O_3$ | 4.00 | 2.27 | 1.97 |
| MnO | 0.07 | 0.05 | 0.00 |
| MgO | 1.61 | 0.93 | 0.53 |
| CaO | 3.22 | 1.15 | 2.18 |
| $Na_2O$ | 3.97 | 3.82 | 3.28 |
| $K_2O$ | 3.01 | 3.69 | 4.08 |
| $P_2O_5$ | 0.22 | 0.12 | 0.00 |
| total | 98.49 | 98.35 | 97.2 |

plagioclase and amphibole, among other minerals (e.g., Chappel et al. 2012). The K/Rb ratio does not significantly increase (approx. 10 to 20% relative) by fractionation of 20 to 30%, as the Rb values only change slightly (10 to 15%), and the K values remain high. However, in Harker diagrams the Griessstein Pluton Rb values are always higher and the Sr values are lower—as expected—compared to the Pletzen Pluton. A slight Eu anomaly is obselvable indicating the proposed plagioclase fractionation. Considering the arguments regarding rhyolite-MELTS calculations described above, as well as the quite similar ages of the Pletzen and Griessstein Pluton (Mandl et al. 2018), we infer that although the Griessstein Pluton geochemically shows, for some portions, S-type character, it genetically evolved from metaluminous I-type melt. Based on the equation of Watson and Harrison (1983), whole-rock zircon saturation temperatures ($T_{Zr}$) were calculated for both plutons of the Hintertal Plutonic Suite. Calculated $T_{Zr}$ of the parental Pletzen Pluton range from 765 to 833 °C with an average of 793 °C. The Griessstein Pluton indicates insignificant lower temperatures ranging from 764 to 814 °C with an average of 788 °C.

The Griessstein Pluton as currently exposed, however, only accounts for approximately 10% of the total Hintertal Plutonic Suite. Either it is just the result of fractionation of small volumes of the original plutonic source, or the Griessstein Pluton intruded at shallower crustal levels and large parts of it were eroded during subsequent uplift of the Variscan Orogen and / or post-Variscan continental rifting. Granitoid components recovered in the Permian clastic meta-sediments of the Rannach Formation have a similar appearance to the Griessstein rocks. Thus, erosion of essential parts of the Griessstein Pluton is rather likely.

### Origin of dikes

Based on chondrite-normalized multi-element variation diagrams two distinct groups of dikes can be distinguished. Dikes of group 1 intruded the metapelites of the Glaneck Metamorphic Suite (MM5 and SP61) but also the Hochreichart Plutonic Suite (MM3, MM69, MM51) and represent highly fractionated melts (Figs. 7, 8 and 10). The pegmatitic dikes (MM5 and SP61) found within the Glaneck Metamorphic Suite show generally higher $TiO_2$, $Al_2O_3$, MgO, CaO, Sr and lower $K_2O$ and Rb values than pegmatitic (MM51), leucogranitic (MM3) and granitic dikes (MM69) penetrating the Hochreichart Plutonic Suite granitiods. U/Pb zircon ages of pegmatitic dikes display concordia ages of 361 ± 13 Ma (MM3) and 365 ± 11 Ma (MM5) (Mandl et al. 2018), which are slightly older compared to the group 2 dikes (see below). The different types of the group 1 dikes represent most likely residual melts from the main stage of the intrusive activity of the Hintertal Plutonic Suite.

Dikes belonging to group 2 (MM14, MM15, MM54) represent evolved granitic melts, similar to the Griessstein Pluton that penetrates mainly the Glaneck Metamorphic Suite. They yield a slightly younger U–Pb zircon age of 348 Ma ± 14 Ma, 331 ± 10 Ma and 349 ± 8 Ma (Mandl et al. 2018) and are interpreted as late fractionation products from the same source region of the Pletzen Pluton, as can be seen by various variation plots e.g., $Al_2O_3$, MgO, $P_2O_5$ vs. $SiO_2$ (Fig. 7a, b, g) as well as e.g., Sr vs. $SiO_2$ and V vs. $SiO_2$ (Fig. 8b, e).

## Paleogeographic setting of the Seckau Complex

### Pre-Variscan evolution

In late Neoproterozoic to Early Cambrian times northern Gondwana destabilized through activity and retreat of the Cadomian Arc. However, the late Cambrian / Ordovician evolution was diachronous in several Peri-Gondwana fragments. Its eastern segments, hosting the future Alpine basement units, experienced short periods of ocean floor formation and re-amalgamated to Gondwana-derived continental blocks in Early Ordovician times (e.g., Frisch et al. 1987; Stampfli et al. 2013; von Raumer et al. 2013, 2015; Cocks and Torsvik 2021). Thus, in this part of the former eastern Gondwana margin, two sutures are thought to exist, an older (Cadomian) suture and a younger suture that formed in Ordovician times. The latter is sometimes referred to as Ceneric suture or Ceneric Orogen (e.g., Zurbriggen 2017; Burda et al. 2021). Remnants of Cambrian / Lower Ordovician short-lived oceanic and rift-related fragments scatter along the Western Alps, Eastern Alps and Carpathians including the Chamrousse ophiolite (Western Alps: ca 500 Ma), the Ötztal and Silvretta gabbros and the Seckau-Schladming metabasites (520–510 Ma), eclogite protolith and arc basalts (ca. 530–490 Ma) south of the Tauern Window and ca. 498 Ma old island-arc related igneous rocks from the Carpathians (for summary see Faryad and Hoinkes 1998; Faryad et al. 2002; Haas et al. 2020; Burda et al. 2021; Huang et al. 2021). Our data from the Hochreichart Suite with 508 ± 9 Ma to 486 ± 9 Ma old arc-related granitoids suggest the existence of a Ceneric active margin with its remnants now exposed in the Seckau Complex. The exact position of this arc segment along a probably Ceneric or Proto-Rheic subduction zone (Burda et al. 2021) expanding from today's North Africa to south China cannot be resolved from our data (Fig. 11a). Considering the age of eclogite facies metamorphism of the Ceneri Complex (Franz and Romer 2007), indicating peak metamorphic conditions of 710 ± 30 °C at 2.1 ± 0.25 GPa, dated by U–Pb zircon and rutile at 457 ± 5 Ma and 443 ± 19 Ma indicating a Late Ordovician age of subduction metamorphism, the Hochreichart Pluton may represent a magmatic arc along the Ceneric active margin (Fig. 11) that predates the closure of the Proto-Rheic ocean.

### Variscan evolution

For the Variscan evolution, two in part contrasting models exist. Kroner and Romer (2013) argue for the existence of a single ocean, the Rheic Ocean (Zulauf 2007), that closed shortly before the Variscan orogeny. In their model many subduction zones evolved within former northern Gondwana, the "Armorican Spur", but most of them are considered as intracontinental subduction zones. Another group of authors (Stampfli et al. 2002, 2013; von Raumer et al. 2013, 2015; Franke et al. 2017) favor the existence of microcontinents (Hun or Galatia Terranes) that amalgamated by closure of multiple, probably small oceanic basins. Since remnants of related ophiolites are not preserved within the Seckau Complex we hardly can support one of those assumptions. However, we can confirm the existence of related early to mid-Variscan (365 ± 8 Ma to 343 ± 12 Ma) plutons with calc-alkaline meta- to peraluminous (Pletzen Pluton) and peraluminous character (Griessstein Pluton) (the term "mid Variscan" in this context refers to von Raumer and Stampfli 2008). These are interpreted to represent arc granitoids corresponding to the early Variscan "Cordillerian" I-type suite. Those granitoids scatter all over the Variscan belt and occur within the northern Saxothuringian (Odenwald), in Central Bohemia (Central Bohemian Batholith; Košler and Farrow 1994; Zák et al. 2011) and the intra-Alpine realm (e.g., eastern part of the Hohe Tauern Batholith, Schladming Batholith) (e.g., Finger et al. 1997). Granitoids with similar geochemical characteristics ("Cetic granitoids") also occur, as

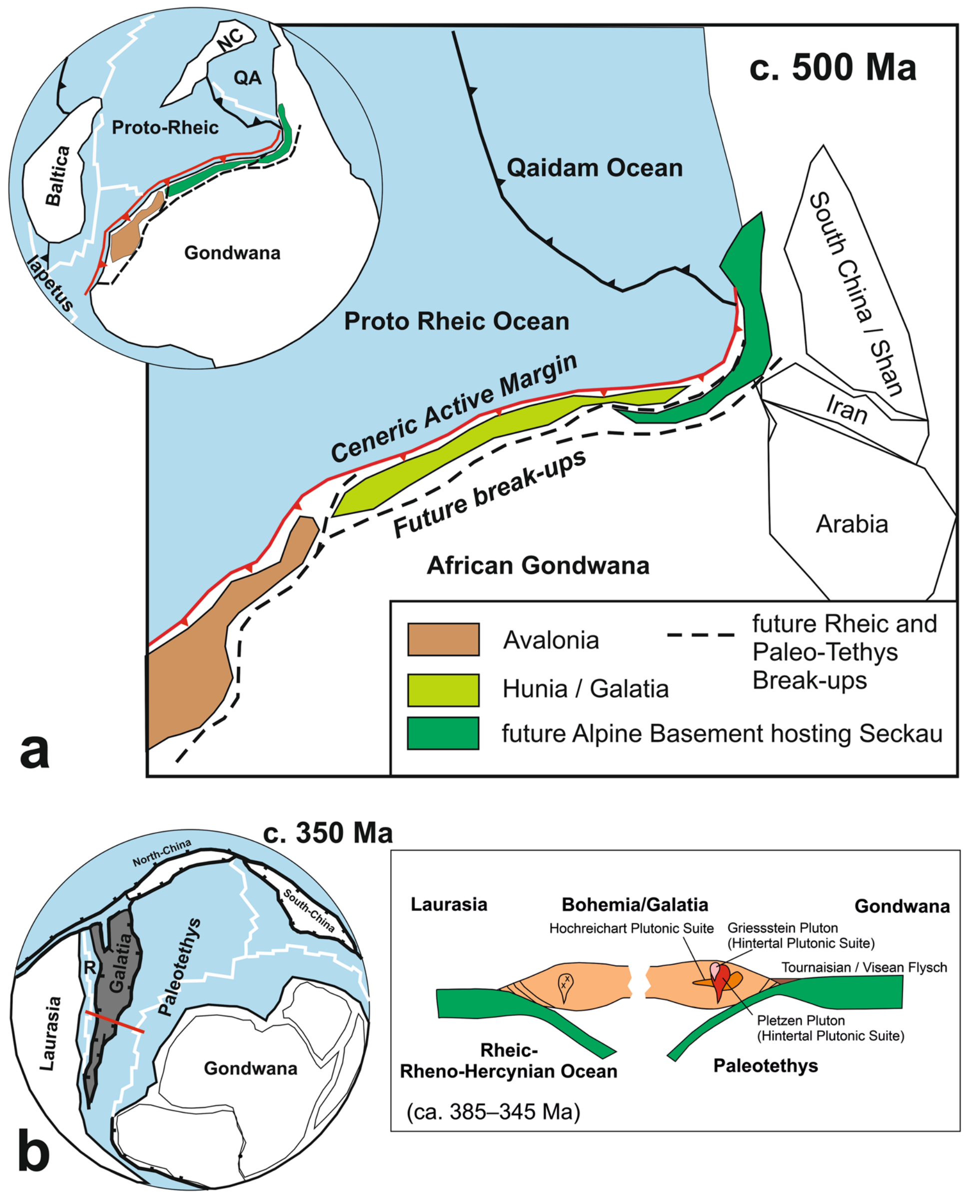


**Fig. 11** **a**) Late Cambrian – Early Ordovician plate tectonic situation. Future Alpine Basement hosting Seckau magmatic suites are located along the Ceneric active margin (modified after Burda et al. 2021). **b**) Late Devonian – Tournaisian plate tectonic situation and cross section across Galatia microcontinent with bipolar subduction of Paleotethys and Rheic—Rheno-Hercynian (R) oceans (modified after Haas et al. 2020)

exotic fragments, along the southern margin of the Bohemian Massif, close to the northern front of the Eastern Alps. The so-called "Cetic granitoids" are embedded in sediments of the Ultrahelvetic and the Rheno-Danubian Flysch Belt and are considered to be part of the Cetic Massif, a hypothetical crystalline basement block which adjoins the Moldanubian Unit to the south and underneath the Eastern Alps (Finger et al. 1997). Considering the fact that the intra-Alpine, early Variscan arc granitoids occur far to the south of the classic ophiolite-decorated Rheic suture, expanding from the British Lizard Complex to the Mid-German Phyllite Zone, we argue for the existence of multiple arcs and closure of multiple oceanic basins. This is supported by findings of early Variscan ca. 370 Ma old meta-ophiolites in the Alpine Carpathian realm (Putis et al. 2009; Burda et al. 2021). Subsequently, in Tournaisian to Visean (Mississippian) times, flysch type sediments were deposited within low-grade metamorphosed fossiliferous units, presently exposed in the Eastern Alps (Hubmann et al. 2013). Flysch sediments overlie passive continental margin sedimentary sequences that were deposited either on the northern Gondwana margin (e.g., Neubauer and Handler 2000) or on the southern rim of Galatia (e.g., Haas et al. 2020). These data suggest a model with double-sided subduction, the southern of which has northward polarity and dips below the Galatia fragment (von Raumer et al. 2013). The general paleogeographic position of the Seckau Complex during the Variscan orogenic phase is considered to be south to southeast of the Bohemian Massif, proximal to the eastern Hohe Tauern, the Schladming Tauern, and the Western Carpathians (Schermaier et al. 1997). Granitoid emplacement can be related to the closure of differently termed oceanic domains (Galicia-Moldanubian Ocean or Paleotethys: Paleotethys in Fig. 11b).

## Conclusions

There is wide consensus that pre-Alpine crustal blocks now distributed within the Eastern Alps derived from the former northern Gondwana margin. However, magmatic and tectonic phases that cover a time range from Cambrian Gondwana destabilization to Pangea formation remained unresolved so far. As the metagranitoids of the Seckau Complex are part of both late Cambrian to Early Ordovician and Late Devonian to Mississipian (early Variscan) intrusive complexes, a re-evaluation of the magmatic and geochemical pre-Alpine evolution of this part of the Eastern Alps is required. Our geochemical data, together with previously published age data, allow the reconstruction of these phases.

The Late Cambrian to Early Ordovician metagranitoids of the Hochreichart Plutonic Suite can be classified as part of a magmatic arc system along the northern Gondwana margin. Calcalkaline suites developed above the southward subducting Prototethys ocean. Retreat of this arc opened short – living oceanic basins (now preserved, e.g., in the Speik Complex; Neubauer 1988; Neubauer et al. 1989; Neubauer and Frisch 1993) that may have been closed shortly after their formation.

In the Middle Ordovician continental slivers succeeded to rift off the northern Gondwana margin through opening of the Paleotethys. This ocean closed during Devonian – Early Carboniferous times including the formation of a second magmatic arc system at c. 350 Ma, represented by the meta- to peraluminous Hintertal Plutonic Suite. The early Variscan granitoids of the Seckau Complex are interpreted as part of an active margin that evolved to the south of today's Bohemia and the Hohe Tauern. Final collision between Gondwana and Laurussia formed late Variscan granitoids now exposed in the western Tauern Window, the European basement of the Swiss Alps (e.g. Aar Massif) and the Bohemian Massif.

**Supplementary information** The online version contains supplementary material available at https://doi.org/10.1007/s00710-022-00781-3.

**Acknowledgements** The authors would like to thank Walter Gössler for providing access to the inductively coupled plasma mass spectrometer (ICP-MS) at the Institute of Chemistry, University of Graz. The authors thank who Fritz Finger brought in his great expertise on the Variscan plutonism during extensive discussions, and highly appreciate the reviews and constructive comments on the first and second manuscript version by Franz Neubauer and Theo Ntaflos.

**Author contribution** All authors contributed to the study conception and design. Material preparation, data collection and analysis were performed by Magdalena Mandl. The first draft of the manuscript was written by Magdalena Mandl and all authors commented on previous versions of the manuscript. All authors read and approved the final manuscript.

**Funding** Open access funding provided by University of Graz.

**Availability of data and materials** All data presented in the text of the article are fully available without restriction from authors upon request. Code availability is not applicable.

## Declarations

**Ethics approval** This study follows the 'European Code of Conduct for Research Integrity ' as well as the 'Ethics for Researchers' guideline of the European Commission.

**Consent to participate** All authors consent to participate on this study.

**Consent for publication** All authors consent for publication of this study.

**Conflicts of interest** No conflicts of interest/No competing interests.



## References

Ballèvre M, Marchand J, Godard G, Goujou J-C, Christian J, Wyns R (1994) Eo-Hercynian events in the Armorican Massif. In: Keppie JD (ed) Pre-Mesozoic Geology in France and Related Areas. Springer, Berlin, pp 183–194

Broska I, Uher P (2001) Whole-rock chemistry and genetic typology of the West-Carpathian Variscan granitoids. Geol Carpath 52(2):79–90

Burda J, Klötzli U, Majka J, Chew D, Li Q-L, Liu Y, Gawęda A, Wiedenbeck M (2021) Tracing proto-Rheic - Qaidam Ocean vestiges into the Western Tatra Mountains and implications for the Palaeozoic palaeogeography of Central Europe. Gondwana Res 91:188–204. https://doi.org/10.1016/j.gr.2020.12.016

Cerńy P (1982) Petrogenesis of granitic pegmatites. In: Cerńy P (ed) Granitic Pegmatites in Science and Industry. Mineral Assoc of Can, Short Course Handb 8:405–461

Chappel BW, White AJR (2001) Two contrasting granite types: 25 years later. Aust J of Earth Sci 48:489–500

Chappel BW, Bryant CJ, Wyborn D (2012) Peraluminous I-type granites. Lithos 153:142–153. https://doi.org/10.1016/j.lithos.2012.07.008

Cocks LRM, Torsvik TH (2021) Ordovician palaeogeography and climate change. Gondwana Res 2021 (in press). https://doi.org/10.1016/j.gr.2020.09.008

Eichhorn R, Loth G, Höll R (2000) Multistage Variscan magmatism in the central Tauern Window (Austria) unveiled by U/Pb SHRIMP zircon data. Contrib Min Petrol 139:418–435

Faryad SW, Hoinkes G (1998) Correlation of metamorphic P-T conditions between basement rocks in the Austro-Alpine units east from the Tauern Window and in the eastern sector of the Western Carpathians. XVI Congress, Carpathian Balkan Geological Association. Abstracts 159

Faryad SW, Hoinkes G (2001) Alpine Chloritoid and Garnet from the Hochgrössen Massif (Speik Complex, Eastern Alps). Mitt Österr Geol Ges 146:387–396

Faryad SW, Hoinkes G (2003) P-T gradient of Eo-Alpine metamorphism within the Austroalpine basement units east of the Tauern Window (Austria). Mineral Petrol 77:129–159

Faryad SW, Melcher F, Hoinkes G, Puhl J, Meisel T, Frank W (2002) Relics of eclogite facies metamorphism in the Austroalpine basement, Hochgrössen (Speik complex), Austria. Mineral Petrol 74:49–73

Finger F, Gerdes A, Janoušek V, René M, Riegler G (2007) Resolving the Variscan evolution of the Moldanubian sector of the Bohemian Massif: the significance of the Bavarian and the Moravo-Moldanubian tectonometamorphic phases. J Geosci 52:9–28

Finger F, Gerdes A, Janoušek V, René M, Riegler G (2009) The Saxo-Danubian Granite Belt: magmatic response to post-collisional delamination of mantle lithosphere below the south-western sector oft he Bohemian Massif (Variscan orogen). Geol Carpath 60:205–212

Finger F, Roberts MP, Haunschmid B, Schermaier M, Steyrer HP (1997) Variscan granitoids of central Europe: their typology, potential sources and tectonothermal relations. Mineral Petrol 61:67–96

Finger F, Broska I, Haunschmid L, Hrasko L, Kohút M, Krenn E, Petrík I, Riegler G, Uher P (2003) Electron-microprobe dating of monazites from Western Carpathian basement granitoids: plutonic evidence for an important Permian rifting event subsequent to Variscan crustal anatexis. Int J of Earth Sci 92:86–98

Flügel HW, Neubauer FR (1984) Geologische Karte der Steiermark 1:200.000. Geologische Bundesanstalt, Wien

Franěk J, Schulmann K, Lexa O, Tomek Č, Edel J-B (2011) Model of syn-convergent extrusion of orogenic lower crust in the core of the Variscan belt: implications for exhumation of high-pressure rocks in large hot orogeny. J Metamorph Geol 29:53–78

Frank W (1987) Evolution of the Austroalpine elements in the Cretaceous. In: Flügel HW, Faupl P (Eds) Geodynamics of the Eastern Alps. Deuticke, Vienna, pp 379–406

Franke W (1989) Tectonostratigraphic units in the Variscan belt of Central Europe. Geol Soc Am Spec Pap 230:67–87

Franke W (2000) The mid-European segment of the Variscides: tectonostratigraphic units, terrane boundaries and plate tectonic evolution. In: Franke W, Haak V, Oncken O, Tanner D (Eds) Orogenic Processes: Quantification and Modelling in the Variscan Belt. Geol Soc Lond Spec Publ 179:35–61

Franke W, Cocks LRM, Torsvik TH (2017) The Palaeozoic Variscan oceans revisited. Gondwana Res 48:257–284

Franke W, Żelaźniewicz A (2002) Structure and evolution of the Bohemian Arc. Geol Soc Lond Spec Publ 201:279–293

Franz L, Romer RL (2007) Caledonian high-pressure metamorphism in the Strona-Ceneri Zone (Southern Alps of southern Switzerland and northern Italy). Swiss J Geosci 100:457–467

Frasl G, Finger F (1988) The „Cetic Massif" below the Eastern Alps – characterized by its granitoids. Schweiz Mineral Petrogr Mitt 68:433–439

Frisch W, Neubauer F, Bröcker M, Brückmann W, Haiss N (1987) Interpretation of geochemical data from the Caledonian basement within the Austroalpine basement complex. In: Flügel HW, Sassi FP, Grecula P (Eds) Pre-Variscan and Variscan Events in the Alpine-Mediterranean Mountain Belts. Mineralia Slovaca-Monograph, Alfa, Bratislava, pp 209–226

Froitzheim N, Schmid SM, Frey M (1996) Mesozoic paleogeography and the timing of eclogite-facies metamorphism in the Alps: A working hypothesis. Eclogae Geol Helv 89:81–110

Froitzheim N, Plasienka D, Schuster R (2008) Alpine tectonics of the Alps and Western Carpathians. In: McCann T (Ed) The Geology of Central Europe Volume 2: Mesozoic and Cenozoic. Geol Soc Lond 1141–1232

Gaab AS, Poller U, Janák M, Kohút M, Todt W (2005) Zircon U-Pb geochronology and isotopic characterization for the pre-Mesozoic basement of the Northern Veporic Unit (Central Western Carpathians, Slovakia). Schweiz Mineral Petrogr Mitt 85:69–88

Gaidies F, Abart R, De Capitani C, Schuster R, Connolly JAD, Reusser E (2006) Characterization of polymetamorphism in the Austroalpine basement east of the Tauern Window using garnet isopleth thermobarometry. J Metamorph Geol 24:451–475

Gómez-Barreiro J, Wijbrans JR, Castiñeiras P, Martínez Catalán JR, Arenas R, Díaz García F, Abati J (2006) $^{40}$Ar/$^{39}$Ar laser probe dating of mylonitic fabrics in a polyorogenic terrane of NW Iberia. J Geol Soc Lond 163:61–73

Gómez Barreiro J, Martínez Catalán JR, Arenas R, Castiñeiras P, Abati J, Díaz García F, Wijbrans JR (2007) Tectonic evolution of the upper allochthon of the Órdenes Complex (northwestern Iberian Massif): Structural constraints to a polyorogenic peri-Gondwanan terrane. Geol Soc Am Spec Pap 423:315–332

Gualda GAR, Ghiorso MS, Lemons RV, Carley TL (2012) Rhyolite-MELTS: A modified calibration of MELTS optimized for silica-rich, fluid-bearing magmatic systems. J Petrol 53:875–890

Haas I, Eichinger S, Haller D, Fritz H, Nievoll J, Mandl M, Hippler D, Hauzenberger C (2020) Gondwana fragments in the Eastern Alps: A travel story from U/Pb zircon data. Gondwana Res 77:204–222. https://doi.org/10.1016/j.gr.2019.07.015

Huang Q, Genser J, Liu Y, Neubauer F, Yuan S, Bernroider M, Guan Q, Jin W, Yu S, Chang R (2021) Cambrian-Ordovician continental magmatic arc at the northern margin of Gondwana: Insights from the Schladming Complex (Eastern Alps). Lithos 388–389. https://doi.org/10.1016/j.lithos.2021.106064

Hubmann B, Ebner F, Ferretti A, Histon K, Kido E, Krainer K, Neubauer F, Schonlaub HP, Suttner TJ (2013) The Paleozoic Era(them). In: Piller WE (ed) The lithostratigraphic units of the Austrian Stratigraphic Chart 2004 (sedimentary successions). Abh der Geol Bundesanst 66:9–133

Irvine TN, Baragar WRA (1971) A guide to the chemical classification of the common volcanic rocks. Can J Earth Sci 8:523–548

Košler J, Farrow CM (1994) Mid-Late Devonian arc-type magmatism in the Bohemian Massif: Sr an Nd isotope and trace element evidence from the Stare Sedlo and Mirotice Gneiss Complex, Czech Republic. J Czech Geol Soc 39:56–57

Kroner U, Romer RL (2013) Two plates — Many subduction zones: the Variscan orogeny reconsidered. Gondwana Res 24:298–329

London D (2008) Pegmatites. Can Mineral, Spec Pub 10:347

Mandl M, Kurz W, Hauzenberger C, Fritz H, Klötzli U, Schuster R (2018) Pre-Alpine evolution of the Seckau Complex (Austroalpine basement/Eastern Alps): Constraints from in-situ LA-ICP-MS U-Pb zircon geochronology. Lithos 296–299:412–430

McDonough WF, Sun S-S (1995) The composition of the Earth. Chem Geol 120:223–253

Metz K (1967) Geologische Karte der Republik Österreich 1:50.000, Blatt 130–131 (Oberzeiring-Kalwang). Geologische Bundesanstalt, Wien

Metz K (1976) Der Geologische Bau der Seckauer und Rottenmanner Tauern. Jahrb Geol Bundesanst 119:151–205

Middlemost EAK (1994) Naming materials in magma/igneous rock system. Earth-Sci Rev 37:215–224

Neubauer F (1988) Bau und Entwicklungsgeschichte des Rennfeld-Mugel- und des Gleinalm-Kristallins (Ostalpen). Abh Geologischen Bundesanst 42:1–137

Neubauer F (1994) Kontinentkollision in Den Ostalpen Geowissenschaften 12:136–140

Neubauer F, Frisch W, Schmerold R, Schlöser H (1989) Metamorphosed and dismembered ophiolite suites in the basement units of the Eastern Alps. Tectonophysics 164:49–62

Neubauer F, Frisch W (1993) The Austroalpine metamorphic basement east of the Tauern Window. In: von Raumer JF, Neubauer F (eds) Pre-Mesozoic Geology of the Alps. Springer, Berlin, pp 551–536

Neubauer F, Handler R (2000) Variscan orogeny in the Eastern Alps and Bohemian Massif: How do these units correlate. Mitt Österr Geol Ges 92:35–59

Pearce J, Harris N, Tindle A (1984) Trace elements discrimination diagrams for the tectonic interpretation of granitic rocks. J Petrol 25:956–983

Peccerillo A, Taylor SR (1976) Geochemistry of Eocene calc-alkaline volcanic rocks from the Kastamonu area, northern Turkey. Contrib Mineral Petrol 58:63–81

Pfingstl S, Kurz W, Schuster R, Hauzenberger C (2015) Geochronological constraints on the exhumation of the Austroalpine Seckau Nappe System (Eastern Alps). Austrian J Earth Sci 108:172–185

Putiš M, Ivan P, Kohút M, Spišiak J, Siman P, Radvanec M, Uher P, Sergeev S, Larionov A, Méres Š, Demko R, Ondrejka M (2009) Meta-igneous rocks of the West-Carpathian basement, Slovakia: indicators of Early Paleozoic extension and shortening events. Bull Soc Géol Fr 180:461–471. https://doi.org/10.2113/gssgfbull.180.6.461

Quemeneur J, Lagache M (1999) Comparative study of two pegmatitic fields from Minas Gerais, Brazil, using the Rb and Cs contents of micas and feldspars. Revista Brasileira De Geociências 29:27–32

Santallier D, Lardeaux JM, Marchand J, Marignac C (1994) The Massif Central, metamorphism. In: Keppie JD (ed) Pre-Mezozoic geology in France and related areas. Springer, Berlin, pp 324–340

Schaltegger U (1990) The central Aar Granite, highly differentiated calc-alkaline magmatism in the Aar Massif (Central Alps, Switzerland). Eur J Mineral 2:234–259

Schermaier A, Haunschmid B, Finger F (1997) Distribution of Variscan I- and S-type granites in the Eastern Alps: a possible clue to unravel pre Alpine basement structures. Tectonophysics 272:315–333

Schmid SM, Fügenschuh B, Kissling E, Schuster R (2004) Tectonic map and overall architecture of the Alpine orogen. Eclogae Geol Helv 97:93–117

Schuster R (2003) Das eo-Alpine Ereignis in den Ostalpen: Plattentektonoische Situation und interne Struktur des Ostalpinen Kristallins. Geologische Bundesanstalt, Arbeitstagung: Blatt 148 Brenner

Schuster R, Kurz W, Krenn K, Fritz H (2013) Introduction to the Geology of the Alps. Ber der Geol Bundesanst 99:121–135

Shand SJ (1943) Eruptive Rocks. John Wiley, New York

Stampfli GM, Hochard C, Verard C, Wilhem C, von Raumer J (2013) The formation of Pangea. Tectonophysics 593:1–9

Stampfli GM, von Raumer J, Borel G (2002) The Paleozoic evolution of pre-Variscan terranes: from Gondwana to the Variscan collision. In: Martinez Catalan JR, Hatcher Jr. RD, Arenas R, Diaz Garcia F (Eds.) Variscan–Appalachian Dynamics: the Building of the Late Paleozoic Basement. Geol Soc Am Spec Pap 364:263–280

Taylor SR, McLennan SM (1985) The Continental Crust: Its Composition and Evolution. Blackwell, Oxford

von Raumer J, Stampfli GM (2008) The birth of the Rheic Ocean—early Palaeozoic subsidence patterns and tectonic plate scenarios. Tectonophysics 461:9–20

von Raumer J, Stampfli GM, Arenas R, Martinez SS (2015) Ediacaran to Cambrian oceanic rocks of the Gondwana margin and their tectonic interpretation. Int J Earth Sci 104. https://doi.org/10.1007/s00531-015-1142-x

von Raumer JF, Bussy F, Schaltegger U, Schulz B, Stampfli GM (2013) Pre-Mesozoic Alpine basements - Their place in the European Paleozoic framework. Geol Soc Am Bull 125:89–108

von Raumer JF, Neubauer F (eds) (1993) The Pre- Mesozoic Geology in the Alps. Springer, Berlin, p 677.

Watson EB, Harrison TM (1983) Zircon saturation revisited: temperature and composition effects in a variety of crustal magma types. Earth Planetary Sci Lett 64:295–304

Whitney DL, Evans BW (2010) Abbreviations for names of rock-forming minerals. Am Mineral 95:185–187

Yuan S, Neubauer F, Liu Y et al (2020) Widespread Permian Granite Magmatism in Lower Austroalpine Units: Significance for Permian Rifting in the Eastern Alps: Swiss J Geosci 113:18. https://doi.org/10.1186/s00015-020-00371-5

Zák J, Kratinová Z, Trubač J, Janoušek V, Sláma J, Mrlina J (2011) Structure, emplacement and tectonic setting of Late Devonian granitoid plutons in the Teplá-Barrandian unit, Bohemian Massif. Int J Earth Sci 100:1477–1495

Zulauf G (2007) The evolution of the Rheic Ocean: From Avalonian-Cadomian active margin to Alleghenian-Variscan collision. Geol Soc Am Spec Pap 423:315–332

Zurbriggen R (2017) The Cenerian orogeny (early Paleozoic) from the perspective of the Alpine region. Int J Earth Sci 106:517–529. https://doi.org/10.1007/s00531-016-1438-5